

APPROXIMATING MATRIX EIGENVALUES BY SUBSPACE ITERATION WITH REPEATED RANDOM SPARSIFICATION*

SAMUEL M. GREENE[†], ROBERT J. WEBBER[‡], TIMOTHY C. BERKELBACH^{†§}, AND JONATHAN WEARE^{‡¶}

Abstract. Traditional numerical methods for calculating matrix eigenvalues are prohibitively expensive for high-dimensional problems. Iterative random sparsification methods allow for the estimation of a single dominant eigenvalue at reduced cost by leveraging repeated random sampling and averaging. We present a general approach to extending such methods for the estimation of multiple eigenvalues and demonstrate its performance for several benchmark problems in quantum chemistry.

Key words. eigenvalues, subspace iteration, randomized algorithms, Monte Carlo

AMS subject classifications. 65F15, 68W20, 65C05

1. Introduction. A wide range of applications, including principal component analysis [63, 2], spectral analysis of dynamical systems [41, 62], and electronic structure calculations [30, 4], require matrix eigenvectors and eigenvalues. Methods for calculating them based on dense, in-place factorizations are intractably expensive for large matrices [57, 58]. Iterative methods involving repeated matrix-vector multiplications [33, 17, 51] offer reduced computational and memory costs, particularly for sparse matrices. However, even these methods are too expensive for the extremely large matrices increasingly encountered in modern applications.

We consider a class of randomized iterative techniques that enable significant further reductions in memory and computational costs. These techniques build on classical iterative methods for solving eigenvalue problems by randomly perturbing vectors or matrices at each iteration to increase sparsity. The imposed sparsity facilitates the use of sparse linear algebra frameworks for performing matrix-vector multiplication efficiently. Because they do not involve storing or manipulating dense vectors, iterative random sparsification methods are particularly suited to problems for which the memory required to store even a single dense vector precludes the application of conventional iterative methods [34]. For singular value decomposition or symmetric eigenvalue decomposition of large matrices, iterative random sparsification methods can have significantly lower computational costs [28, 34, 36, 3, 44] than methods that start with a random matrix and repeatedly apply dense matrix multiplications [48, 26, 27, 24, 39].

When used to estimate the ground-state energy, or smallest eigenvalue, of the quantum mechanical Hamiltonian operator, iterative random sparsification methods

*Submitted to the editors DATE.

Funding: S.M.G. is supported by an investment fellowship from the Molecular Sciences Software Institute, which is funded by U.S. National Science Foundation grant OAC-1547580. R.J.W. is supported by New York University’s Dean’s Dissertation Fellowship and by the National Science Foundation through award DMS-1646339. J.W. acknowledges support from the Advanced Scientific Computing Research Program within the DOE Office of Science through award DE-SC0020427. The Flatiron Institute is a division of the Simons Foundation.

[†]Department of Chemistry, Columbia University, New York, New York 10027, United States.

[‡]Courant Institute of Mathematical Sciences, New York University, New York, New York 10012, United States.

[§]Center for Computational Quantum Physics, Flatiron Institute, New York, New York 10010, United States (tim.berkelbach@gmail.com).

[¶]weare@cims.nyu.edu

are termed “projector quantum Monte Carlo” methods [40, 15, 36, 38, 22, 23]. These methods have become a standard tool for calculating ground-state electronic energies of molecules. Applying such methods to calculate *multiple* eigenvalues poses additional challenges related to the need to maintain orthogonality among eigenvectors as the iteration proceeds [11, 42, 7, 19]. Yet successful extension to the multiple eigenvalue problem would have implications not only for quantum applications, but in other areas of physics, engineering, and data science.

This article presents a subspace iteration approach with repeated random sparsification for estimation of multiple dominant eigenvalues. This approach is based on a version of subspace iteration with several non-standard design choices to increase the method’s stability under random perturbations. Random perturbations are introduced to the vectors at each iteration to promote sparsity, and we prove that our approach to random sparsification is as efficient as possible: it minimizes the mean square error in the vector entries while ensuring sparsity and preserving the original vector in expectation. The resulting subspace iteration with repeated random sparsification is similar to approaches for calculating the single dominant eigenvalue within the fast randomized iteration framework [34, 36, 22, 23], but the random sparsification technique is new, and the extension from estimating one dominant eigenvalue to multiple dominant eigenvalues is a fundamentally new feature with broad applicability. We test our method on the full configuration interaction eigenproblem from many-electron quantum mechanics; in this context, it can be understood as a generalization of projector Monte Carlo methods to excited states.

After motivating and introducing the new algorithm, we present numerical tests demonstrating that it reduces per-iteration computational costs compared to deterministic subspace iteration and yields accurate eigenvalue estimates after sufficiently many iterations. Whereas the errors in deterministic subspace iteration shrink exponentially fast with a rate determined by an appropriate eigenvalue ratio, the randomized algorithm gives noisier results, which necessitates averaging over multiple iterations to reduce error. A theoretical analysis validates an *a posteriori* variance estimator to measure the convergence rate for the randomized scheme. Although there can be a small discrepancy between the converged eigenvalue estimates and the true eigenvalues that is not captured by our variance estimator, the high quality of the eigenvalue estimates in our numerical tests and the potential for dramatic cost-savings make our method deserving of further theoretical and algorithmic development, especially as it is scaled up to larger systems.

The remainder of this paper begins with a description of the deterministic subspace iteration method on which our randomized algorithm is based, with a particular focus on its non-standard features that make it amenable to randomization (Section 2). Section 3 describes our approach to stochastically imposing sparsity in vectors and matrices. Section 4 describes our randomized subspace iteration scheme. Section 5 presents a theoretical error analysis. Section 6 presents applications of this algorithm to quantum mechanical problems. In Section 7, we summarize our key findings and discuss possible methodological improvements.

Throughout this work, we use the following notation:

- Matrices \mathbf{X} are written in bold capital letters, vectors \mathbf{x} are written in bold lower case letters, and scalars x are written in italic lower case letters.
- We use \mathbf{x}_i to indicate the i^{th} entry of a vector, \mathbf{X}_{ij} to indicate the (i, j) entry of a matrix, and $\mathbf{X}_{:,i}$ to indicate the i th column of a matrix.
- For any vector $\mathbf{x} \in \mathbb{R}^n$, $\|\mathbf{x}\|_2 = (\sum_{i=1}^n |\mathbf{x}_i|^2)^{1/2}$ denotes the Euclidean norm, $\|\mathbf{x}\|_1 = \sum_{i=1}^n |\mathbf{x}_i|$ denotes the sum of the absolute values of the entries, and

- $\|\mathbf{x}\|_0 = \sum_{i=1}^n \mathbb{1}\{\mathbf{x}_i \neq 0\}$ denotes the number of nonzero entries.
- $\mathbf{X}|_S$ signifies the restriction of a matrix \mathbf{X} to a linear subspace S , while \mathbf{P}_S and $\mathbf{P}_{\mathbf{X}}$ signify orthogonal projections onto a linear subspace S or the column span of a matrix \mathbf{X} .
- Lastly, \mathbb{E} , \mathbb{P} , Var , and Cov indicate expectations, probabilities, variances, and covariances with respect to a probability space that is sufficiently rich to support all the random variables identified in the analysis.

2. A non-standard deterministic subspace iteration. Our goal is to find the k dominant eigenvalues (counting multiplicity) of a matrix $\mathbf{A} \in \mathbb{R}^{n \times n}$. Starting from an initial matrix $\mathbf{X}^{(0)} \in \mathbb{R}^{n \times k}$, standard subspace iteration techniques construct a sequence of “matrix iterates” according to the iteration

$$(2.1) \quad \mathbf{X}^{(i+1)} = \mathbf{A}\mathbf{X}^{(i)}[\mathbf{G}^{(i)}]^{-1},$$

where multiplication by $[\mathbf{G}^{(i)}]^{-1}$ enforces orthonormality among the columns of $\mathbf{X}^{(i+1)}$ [56, 55, 49]. For $k = 1$, subspace iteration reduces to power iteration, on which many single-eigenvalue randomized iterative methods are based. For $k > 1$ (the case considered here), subspace iteration provides a solution to the multiple dominant eigenvalue problem. Eigenvalues of \mathbf{A} can be estimated after each iteration by solving the eigenvalue problem

$$(2.2) \quad \mathbf{X}^{(i)*} \mathbf{A} \mathbf{X}^{(i)} \mathbf{W}^{(i)} = \mathbf{W}^{(i)} \mathbf{\Lambda}^{(i)}$$

for the diagonal matrix $\mathbf{\Lambda}^{(i)}$ of eigenvalue estimates [56].

Standard subspace iteration involves nonlinear operations on the iterates, both for estimating eigenvalues as in (2.2) and for enforcing orthonormality of columns. However, these operations lead to statistical biases once randomness is introduced into the iterates by stochastic sparsification. In order to reduce these errors in our randomized algorithm, we make two non-standard choices.

As a first non-standard choice, we estimate eigenvalues by solving the eigenvalue problem

$$(2.3) \quad \mathbf{U}^* \mathbf{A} \mathbf{X}^{(i)} \mathbf{W}^{(i)} = \mathbf{U}^* \mathbf{X}^{(i)} \mathbf{W}^{(i)} \mathbf{\Lambda}^{(i)},$$

where \mathbf{U} is a constant deterministic matrix with columns chosen to approximate the dominant eigenvectors of \mathbf{A} . Equation (2.3) represents a multi-eigenvalue generalization of the “projected estimator” commonly used in single-eigenvalue randomized methods [10]. Here, we also use the eigenvector estimates \mathbf{U} as the first iterate, i.e. $\mathbf{X}^{(0)} = \mathbf{U}$.

Ideally, the matrix \mathbf{U} should be chosen to span the subspace of the dominant k eigenvectors as nearly as possible, both to ensure a reasonable starting point and to optimize eigenvalue accuracy at every subsequent iteration. Indeed, eigenvalue estimates are exact for any eigenvector exactly contained within the column span of \mathbf{U} . Explicit error bounds that reveal the importance of choosing a good starting matrix \mathbf{U} are stated and proved in Section 5.1.

As a second non-standard choice, we construct the matrices $\mathbf{G}^{(i)}$ in an unusual way. For most iterations i , we construct $\mathbf{G}^{(i)}$ to be a diagonal matrix that controls the scaling of the columns of $\mathbf{X}^{(i+1)}$. Specifically, we most often set $\mathbf{G}^{(i)} = \mathbf{N}^{(i)}$, where $\mathbf{N}^{(i)}$ is a diagonal matrix with elements

$$(2.4) \quad \mathbf{N}_{jj}^{(i)} = \left(\frac{\|\mathbf{X}_{:j}^{(i)}\|_1}{\|\mathbf{X}_{:j}^{(i-1)}\|_1} \right)^\alpha \left(\mathbf{N}_{jj}^{(i-1)} \right)^{(1-\alpha)}, \quad \mathbf{N}_{jj}^{(0)} = 1,$$

and α is a user-defined parameter. Choosing $\alpha = 1$ keeps the ℓ_1 -norm of each iterate column constant (i.e. $\|\mathbf{X}_{:j}^{(i)}\|_1 = \|\mathbf{X}_{:j}^{(i-1)}\|_1$) but introduces a bias, since $\mathbf{N}^{(i)}$ depends non-linearly on iterates. Choosing $\alpha < 1$ allows one to reduce the bias by damping this non-linear dependence. We found that $\alpha = 0.5$ was a suitable choice for our numerical experiments.

Occasionally, we construct $\mathbf{G}^{(i)}$ to be a non-diagonal matrix that improves the orthogonality of the columns of $\mathbf{X}^{(i+1)}$, by setting $\mathbf{G}^{(i)} = \mathbf{N}^{(i)}\mathbf{D}^{(i)}\mathbf{R}^{(i)}$, where $\mathbf{R}^{(i)}$ is the upper triangular factor from a QR factorization of $\mathbf{U}^*\mathbf{A}\mathbf{X}^{(i)}$ and $\mathbf{D}^{(i)}$ is the diagonal matrix with entries $\mathbf{D}_{jj}^{(i)} = \|(\mathbf{X}^{(i)}[\mathbf{R}^{(i)}]^{-1})_{:j}\|_1 / \|\mathbf{X}_{:j}^{(i)}\|_1$. Multiplication by $[\mathbf{G}^{(i)}]^{-1}$ enforces orthogonality only within the column span of \mathbf{U} rather than in the full vector space.

The interval at which orthogonalization should be performed can be determined by monitoring the condition number of the matrix $\mathbf{U}^*\mathbf{X}^{(i)}$. If orthogonalization is performed too infrequently, the condition number will increase as the iteration proceeds, giving rise to instabilities in the algorithm. We monitored this condition number for each of our calculations (Appendix B) and found $\Delta = 1000$ iterations to be a suitable orthogonalization interval. Orthogonalizing more frequently did not change our results significantly.

The principle motivating these non-standard choices is that non-linear operations in our iteration should typically only be applied to products of a random matrix and a constant matrix (i.e. $\mathbf{U}^*\mathbf{X}^{(i)}$ or $\mathbf{U}^*\mathbf{A}\mathbf{X}^{(i)}$), or to the column norms $\|\mathbf{X}_{:j}^{(i)}\|_1$. This leads to a sub-optimal deterministic algorithm: if \mathbf{A} is symmetric and positive semidefinite, eigenvalues estimated using our non-standard approach have error that decays at a rate $(\lambda_j/\lambda_{k+1})^i$ as $i \rightarrow \infty$, whereas errors using the standard eigenvalue estimator (2.2) decay faster, at a rate $(\lambda_j/\lambda_{k+1})^{2i}$ (Section 5.1). However, when iterates are randomized as described below, their products with deterministic matrices typically have very low bias and variance, even while quadratic forms involving the random iterates (i.e. $\mathbf{X}^{(i)*}\mathbf{A}\mathbf{X}^{(i)}$ or $\mathbf{X}^{(i)*}\mathbf{X}^{(i)}$) are typically very far from their deterministic counterparts [34].

3. Stochastic compression. If sparsity is leveraged, the cost of forming the matrix products $\mathbf{A}\mathbf{X}^{(i)}$ in the above algorithm scales as $\mathcal{O}(m_a m_x k)$, where m_a and m_x are the number of nonzero elements in each column of \mathbf{A} and $\mathbf{X}^{(i)}$, respectively. Stochastic compression allows one to control this cost by zeroing nonzero elements at randomly selected positions. We define a stochastic compression operator Φ which, when applied to a generic vector \mathbf{x} , returns a random compressed vector $\Phi(\mathbf{x})$ with (1) at most a user-specified number m of nonzero elements, and (2) all elements equal to those of the input vector \mathbf{x} in expectation, i.e., $\mathbb{E}[\Phi(\mathbf{x})_i] = \mathbf{x}_i$. Applying Φ to a matrix $\mathbf{X} = [\mathbf{X}_{:1} \ \mathbf{X}_{:2} \ \dots]$ involves compressing each of its columns independently to m nonzero elements, i.e. $\Phi(\mathbf{X}) = [\Phi(\mathbf{X}_{:1}) \ \Phi(\mathbf{X}_{:2}) \ \dots]$.

We provide an example of a possible compression scheme in the remainder of this section. We find that this ‘‘pivotal compression’’ algorithm generally achieves less variance in practice than previous compression schemes [34, 22, 23], and we prove in Section 5.2 that this scheme minimizes the mean square compression error $\mathbb{E}\|\Phi(\mathbf{x}) - \mathbf{x}\|_2^2$ subject to unbiasedness and sparsity constraints, and therefore it has the best mathematical properties of any known compression scheme. Additionally, when m equals or exceeds the number of nonzero elements in \mathbf{x} , pivotal compression yields the exact input vector \mathbf{x} , in which case the statistical error is zero.

The first step in pivotal compression involves identifying a set \mathcal{D} of indices cor-

responding to the d largest-magnitude elements in \mathbf{x} . These elements are preserved exactly during the compression, i.e. $\Phi(\mathbf{x})_i = \mathbf{x}_i$ for all $i \in \mathcal{D}$. The number d is chosen such that

$$(3.1) \quad |\mathbf{x}_i| \geq \frac{1}{m-d} \sum_{j \notin \mathcal{D}} |\mathbf{x}_j|, \quad \forall i \in \mathcal{D},$$

$$(3.2) \quad |\mathbf{x}_i| \leq \frac{1}{m-d} \sum_{j \notin \mathcal{D}} |\mathbf{x}_j|, \quad \forall i \notin \mathcal{D}.$$

The next step is to apply pivotal sampling [18, 12, 13] to randomly sample a set \mathcal{S} consisting of $m-d$ additional indices. The probability that each index i is included in \mathcal{S} is

$$(3.3) \quad \mathbf{p}_i = \frac{(m-d) |\mathbf{x}_i|}{\sum_{j \notin \mathcal{D}} |\mathbf{x}_j|}, \quad \forall i \notin \mathcal{D}.$$

Lastly, the sets \mathcal{D} and \mathcal{S} are used to construct the compressed vector $\Phi(\mathbf{x})$ as

$$(3.4) \quad \Phi(\mathbf{x})_i = \begin{cases} \mathbf{x}_i, & i \in \mathcal{D}, \\ \mathbf{x}_i / \mathbf{p}_i, & i \in \mathcal{S}, \\ 0, & i \notin \mathcal{D}, i \notin \mathcal{S}, \end{cases}$$

thus ensuring that this compression scheme is unbiased (i.e. that $\mathbb{E}\Phi(\mathbf{x}) = \mathbf{x}$). We provide complete pseudocode for performing pivotal compression in Appendix A.1 and discuss a possible approach to parallelizing the exact preservation and random sampling steps of this compression scheme in Appendix A.2.

4. Randomized subspace iteration. Applying stochastic compression to our subspace iteration yields

$$(4.1) \quad \mathbf{X}^{(i+1)} = \mathbf{A}\Phi(\mathbf{X}^{(i)})[\mathbf{G}^{(i)}]^{-1},$$

where the compression operation Φ is performed independently at each iteration. The matrix products $\mathbf{U}^* \mathbf{A}\Phi(\mathbf{X}^{(i)})$ and $\mathbf{U}^* \mathbf{X}^{(i)}$ are evaluated and stored for the purpose of estimating eigenvalues. We provide a complete pseudocode in Algorithm 4.1 below.

In order to produce eigenvalue estimates after running Algorithm 4.1, we first form the matrices

$$(4.2) \quad \langle \mathbf{U}^* \mathbf{A}\Phi(\mathbf{X}^{(i)}) \rangle_i = \frac{1}{i_{\max} - i_{\min}} \sum_{i=i_{\min}}^{i_{\max}-1} \mathbf{U}^* \mathbf{A}\Phi(\mathbf{X}^{(i)}),$$

$$(4.3) \quad \langle \mathbf{U}^* \mathbf{X}^{(i)} \rangle_i = \frac{1}{i_{\max} - i_{\min}} \sum_{i=i_{\min}}^{i_{\max}-1} \mathbf{U}^* \mathbf{X}^{(i)},$$

which are time-averages starting from an initial burn-in time i_{\min} and going until the final time i_{\max} . Then, we solve the eigenvalue equation

$$(4.4) \quad \langle \mathbf{U}^* \mathbf{A}\Phi(\mathbf{X}^{(i)}) \rangle_i \mathbf{W} = \langle \mathbf{U}^* \mathbf{X}^{(i)} \rangle_i \mathbf{W} \Lambda^{(i_{\max})}.$$

From our theoretical analysis in Section 5.3, we anticipate that the time averages (4.2) and (4.3) will converge to ergodic limits as $i_{\max} \rightarrow \infty$, for any fixed value of

Algorithm 4.1 Randomized subspace iteration

```

1: Input: Matrix  $\mathbf{U}$  whose columns approximate the  $k$  dominant eigenvectors of  $\mathbf{A}$ 
2: Initialization:  $\mathbf{X}^{(0)} = \mathbf{U}$  and  $\mathbf{N}^{(0)} = \mathbf{I}$ 
3: for  $i = 0, 1, 2, \dots, i_{\max} - 1$  do
4:    $\mathbf{J}^{(i)} = \mathbf{U}^* \mathbf{X}^{(i)}$ 
5:   Construct  $\mathbf{X}^{(i)'} = \Phi(\mathbf{X}^{(i)})$  ▷ Pivotal compression
6:    $\mathbf{Y}^{(i)} = \mathbf{A} \mathbf{X}^{(i)'}$ 
7:    $\mathbf{K}^{(i)} = \mathbf{U}^* \mathbf{Y}^{(i)}$ 
8:   if  $i \equiv 999 \pmod{1000}$  then
9:     Construct  $\mathbf{Q}^{(i)} \mathbf{R}^{(i)} = \mathbf{K}^{(i)}$  ▷ QR factorization
10:     $\mathbf{Z}^{(i)} = \mathbf{Y}^{(i)} [\mathbf{R}^{(i)}]^{-1}$ 
11:    for  $j = 1, 2, 3, \dots, k$  do
12:       $\mathbf{D}_{jj}^{(i)} = \left\| \mathbf{Z}_{:,j}^{(i)} \right\|_1 \left\| \mathbf{Y}_{:,j}^{(i)} \right\|_1^{-1}$ 
13:    end for
14:     $\mathbf{G}^{(i)} = \mathbf{N}^{(i)} \mathbf{D}^{(i)} \mathbf{R}^{(i)}$ 
15:  else
16:     $\mathbf{G}^{(i)} = \mathbf{N}^{(i)}$ 
17:  end if
18:   $\mathbf{X}^{(i+1)} = \mathbf{Y}^{(i)} [\mathbf{G}^{(i)}]^{-1}$ 
19:  for  $j = 1, 2, \dots, k$  do
20:     $\mathbf{N}_{jj}^{(i+1)} = \left\| \mathbf{X}_{:,j}^{(i+1)} \right\|_1^\alpha \left\| \mathbf{X}_{:,j}^{(i)} \right\|_1^{-\alpha} \left[ \mathbf{N}_{jj}^{(i-1)} \right]^{1-\alpha}$ 
21:  end for
22: end for
23: Return: Sequence of matrices  $\mathbf{J}^{(i)} = \mathbf{U}^* \mathbf{X}^{(i)}$  and  $\mathbf{K}^{(i)} = \mathbf{U}^* \mathbf{A} \Phi(\mathbf{X}^{(i)})$ .

```

the burn-in time $i_{\min} \geq 0$. However, it is beneficial to choose a positive burn-in time $i_{\min} > 0$, which reduces the period of *initialization bias* in which (4.2) and (4.3) systematically deviate from their limiting values [52]. To choose i_{\min} in our numerical experiments, we use the approach of [14], whereby we increase i_{\min} until the autocorrelation times associated with our eigenvalue estimates begin to stabilize (signalling that the period of initialization bias has ended).

Lastly, the analysis in Section 5.3 indicates that the standard error of each eigenvalue estimate $\Lambda_{jj}^{(i_{\max})}$ can be estimated through the formula

$$(4.5) \quad \text{Var}[\Lambda_{jj}^{(i_{\max})}] \approx \frac{1}{(i_{\max} - i_{\min})^2} \sum_{\substack{i_{\min} \leq i, k \leq i_{\max}-1 \\ |i-k| \leq \tau}} \text{Cov} \left[f_j^{(i)}, f_j^{(k)} \right].$$

Here, $f_j^{(i_{\min})}, f_j^{(i_{\min}+1)}, \dots$ is a scalar-valued time series, defined by

$$(4.6) \quad f_j^{(i)} = \mathbf{z}_j^* \left(\mathbf{U}^* \mathbf{Y}^{(i)} - \Lambda_{jj}^{(i_{\max})} \mathbf{U}^* \mathbf{X}^{(i)} \right) \mathbf{w}_j,$$

and \mathbf{z}_k and \mathbf{w}_k represent left and right generalized eigenvectors corresponding to $\Lambda_{jj}^{(i_{\max})}$. The truncation threshold $\tau > 0$ is chosen so that correlations involving $f_j^{(i)}$ and $f_j^{(k)}$ are negligibly small for any $|i - k| > \tau$ [52]. Determining the truncation threshold τ and computing the variance (4.5) are common procedures in the analysis of Markov chain Monte Carlo estimates and are conveniently implemented in the emcee package for python [20], which we use throughout our numerical experiments.

5. Theoretical analysis. A full mathematical analysis of Algorithm 4.1 with explicit error bounds is difficult. Although [34] analyzes the single-vector version of Algorithm 4.1, this analysis assumes that the matrix \mathbf{A} is nonnegative so the dominant eigenvector of \mathbf{A} is nonnegative as well. In contrast, here we compute multiple eigenvalues of general matrices with both positive and negative entries. The cancellation of positive and negative entries when computing matrix-vector products is known as the ‘sign problem’ in computational quantum physics, and it has presented a major obstacle to rigorous analysis of random iterative sparsification algorithms, although there have been some informal efforts to understand the phenomenon better [32, 53].

Instead, in this section we present a thorough analysis of the deterministic scheme presented in Section 2, and argue that the stochastic compression introduced in Section 3 is the best possible one in a specific mathematical sense. Finally, we establish an asymptotic (in the limit of large i_{\max}) expression for the variance in our eigenvalue estimates that can be computed in practical settings to evaluate the performance of the scheme. We defer to our numerical tests in Section 6 to show that our approach is effective on realistic problems and to Appendix C to demonstrate that the same randomization of a more standard subspace iteration fails dramatically.

5.1. Analysis of the deterministic subspace iteration. We derive error bounds for the non-standard deterministic subspace iteration that was presented in Section 2, assuming the matrix $\mathbf{A} \in \mathbb{R}^{n \times n}$ is symmetric. Our derivation is based on the following two useful observations.

The first useful observation is that the iteration (2.1) leads to an explicit representation

$$(5.1) \quad \mathbf{X}^{(i)} = \mathbf{A}^i \mathbf{U} \left[\mathbf{G}^{(i-1)} \mathbf{G}^{(i-2)} \dots \mathbf{G}^{(0)} \right]^{-1}.$$

Therefore, by substituting $\mathbf{V}^{(i)} = \left[\mathbf{G}^{(i-1)} \mathbf{G}^{(i-2)} \dots \mathbf{G}^{(0)} \right]^{-1} \mathbf{W}^{(i)}$ into (2.3), the eigenvalue problem simplifies to become

$$(5.2) \quad \underbrace{\mathbf{U}^* \mathbf{A}^{i+1} \mathbf{U}}_{\text{symmetric matrix}} \mathbf{V}^{(i)} = \underbrace{\mathbf{U}^* \mathbf{A}^i \mathbf{U}}_{\text{symmetric matrix}} \mathbf{V}^{(i)} \boldsymbol{\Lambda}^{(i)},$$

which is a symmetric generalized eigenvalue problem involving matrices $\mathbf{U}^* \mathbf{A}^i \mathbf{U}$ and $\mathbf{U}^* \mathbf{A}^{i+1} \mathbf{U}$.

The second useful observation is that the solutions to the symmetric generalized eigenvalue problem (5.2) are given by the Courant-Fischer min-max principle [47, 45]. At least one of the matrices $\mathbf{U}^* \mathbf{A}^i \mathbf{U}$ and $\mathbf{U}^* \mathbf{A}^{i+1} \mathbf{U}$ is positive semidefinite (depending on whether i is odd or even), and this is enough to guarantee the min-max principle applies [45, sec. 1.7]. Indeed, if eigenvalues are ordered from largest to smallest,

$$(5.3) \quad \boldsymbol{\Lambda}_{11}^{(i)} \geq \boldsymbol{\Lambda}_{22}^{(i)} \geq \dots \geq \boldsymbol{\Lambda}_{kk}^{(i)},$$

then the min-max principle gives the representation

$$(5.4) \quad \boldsymbol{\Lambda}_{jj}^{(i)} = \max_{\substack{S \subseteq \text{range}[\mathbf{U}] \\ \dim[S]=j}} \min_{\mathbf{x} \in S} \frac{\mathbf{x}^* \mathbf{A}^{i+1} \mathbf{x}}{\mathbf{x}^* \mathbf{A}^i \mathbf{x}}, \quad 1 \leq j \leq k, \quad i \geq 0.$$

The min-max representation (5.4) is closely analogous to a variational principle for the eigenvalues of \mathbf{A} , except for the explicit dependence on the starting matrix \mathbf{U} .

If we order the eigenvalues of \mathbf{A} from largest to smallest,

$$(5.5) \quad \lambda_1 \geq \lambda_2 \geq \cdots \geq \lambda_n,$$

then the eigenvalues of \mathbf{A} satisfy

$$(5.6) \quad \lambda_j = \max_{\substack{S \subseteq \mathbb{R}^n \\ \dim[S]=j}} \min_{\mathbf{x} \in S} \frac{\mathbf{x}^* \mathbf{A}^{i+1} \mathbf{x}}{\mathbf{x}^* \mathbf{A}^i \mathbf{x}}, \quad 1 \leq j \leq n, \quad i \geq 0,$$

which is a variation on (5.4) with $\text{range}[\mathbf{U}]$ replaced by the larger space \mathbb{R}^n . Thus, by comparing (5.4) and (5.6) we obtain the inequality

$$(5.7) \quad \Lambda_{jj}^{(i)} \leq \lambda_j,$$

valid for all $1 \leq j \leq k$ and $i \geq 0$.

So far, we have bounded the eigenvalue estimates $\Lambda_{jj}^{(i)}$ from above using the true eigenvalues λ_j . However, the task remains to bound the eigenvalues $\Lambda_{jj}^{(i)}$ from below, which is exactly what we accomplish in the next proposition.

PROPOSITION 5.1. *Let β be a permutation that reorders the eigenvalues of \mathbf{A} by magnitude, i.e.,*

$$(5.8) \quad |\lambda_{\beta(1)}| \geq |\lambda_{\beta(2)}| \geq \cdots \geq |\lambda_{\beta(n)}|,$$

and let H_k be a subspace of eigenvectors of \mathbf{A} with eigenvalues $\lambda_{\beta(1)}, \dots, \lambda_{\beta(k)}$. Let

$$(5.9) \quad \theta = \arccos \left(\min_{\mathbf{x} \in H_k} \frac{\|\mathbf{P}_U \mathbf{x}\|}{\|\mathbf{x}\|} \right)$$

be the angular distance between H_k and $\text{range}[\mathbf{U}]$, and assume $\theta < \frac{\pi}{2}$. Lastly, set

$$(5.10) \quad R = \frac{|\lambda_{\beta(k+1)}|}{\lambda_j}$$

and assume $0 \leq R \leq 1$. Then, the eigenvalue estimates $\Lambda_{jj}^{(i)}$ resulting from the deterministic subspace iteration (2.1) and the eigenvalue equation (2.3) satisfy

$$(5.11) \quad \frac{1 - \tan^2 \theta R^{i+1}}{1 + \tan^2 \theta R^i} \lambda_j \leq \Lambda_{jj}^{(i)} \leq \lambda_j.$$

Proof. The main idea of the proof is to construct a particular subset $S \subseteq \text{range}[\mathbf{U}]$ such that $\dim[S] \geq j$ and

$$(5.12) \quad \frac{\mathbf{x}^* \mathbf{A}^{i+1} \mathbf{x}}{\mathbf{x}^* \mathbf{A}^i \mathbf{x}} \geq \frac{1 - \tan^2 \theta R^{i+1}}{1 + \tan^2 \theta R^i} \lambda_j, \quad \forall \mathbf{x} \in S.$$

Then the Courant-Fischer min-max principle (5.4) guarantees that

$$(5.13) \quad \Lambda_{jj}^{(i)} \geq \frac{1 - \tan^2 \theta R^{i+1}}{1 + \tan^2 \theta R^i} \lambda_j,$$

as claimed.

To build the set S , let $J \subseteq H_k$ be the subspace spanned by eigenvectors of \mathbf{A} with eigenvalues $\lambda_1, \dots, \lambda_j$, and define

$$(5.14) \quad J' = H_k \cap J^\perp, \quad Q_k = \mathbf{P}_U H_k, \quad S' = \mathbf{P}_U J', \quad S = Q_k \cap (S')^\perp.$$

We note for further reference that J and J' form an orthogonal decomposition of H_k , while S and S' form an orthogonal decomposition of Q_k . Moreover, we can immediately identify two important facts about the subspace S .

1. $\dim[S] \geq j$ because S has the same dimensionality as J .
2. For any $\mathbf{x} \in S$ and $\mathbf{y} \in J'$ we must have

$$(5.15) \quad \langle \mathbf{x}, \mathbf{y} \rangle = \langle \mathbf{P}_U \mathbf{x}, \mathbf{y} \rangle = \langle \mathbf{x}, \mathbf{P}_U \mathbf{y} \rangle = 0$$

because \mathbf{x} lies in the range of \mathbf{U} and orthogonal to $\mathbf{P}_U J'$.

The remainder of the proof uses this second fact to obtain bounds on

$$(5.16) \quad \min_{\mathbf{x} \in S} \frac{\mathbf{x}^* \mathbf{P}_J \mathbf{x}}{\|\mathbf{x}\|^2} \quad \text{and subsequently} \quad \min_{\mathbf{x} \in S} \frac{\mathbf{x}^* \mathbf{A}^{i+1} \mathbf{x}}{\mathbf{x}^* \mathbf{A}^i \mathbf{x}}.$$

We begin by checking that

$$(5.17) \quad \min_{\mathbf{x} \in S} \frac{\mathbf{x}^* \mathbf{P}_J \mathbf{x}}{\|\mathbf{x}\|^2} = \min_{\mathbf{x} \in S} \frac{\mathbf{x}^* (\mathbf{P}_J + \mathbf{P}_{J'}) \mathbf{x}}{\|\mathbf{x}\|^2}$$

$$(5.18) \quad = \min_{\mathbf{x} \in S} \frac{\mathbf{x}^* \mathbf{P}_{H_k} \mathbf{x}}{\|\mathbf{x}\|^2}$$

$$(5.19) \quad = \min_{\mathbf{x} \in S} \frac{\|\mathbf{P}_{H_k} \mathbf{x}\|^2}{\|\mathbf{x}\|^2}$$

$$(5.20) \quad \geq \min_{\mathbf{x} \in Q_k} \frac{\|\mathbf{P}_{H_k} \mathbf{x}\|^2}{\|\mathbf{x}\|^2},$$

where (5.17) uses the fact that \mathbf{x} is orthogonal to J' , (5.18) uses the fact that J and J' provide an orthogonal decomposition of H_k , (5.19) uses the fact that $\mathbf{P}_{H_k} = \mathbf{P}_{H_k}^2$, and (5.20) uses the fact that $S \subseteq Q_k$.

To further simplify (5.20), we introduce matrices $\mathbf{H}, \mathbf{Q} \in \mathbb{R}^{n \times k}$ with orthogonal columns that span the subspaces H_k and Q_k respectively. Using the variational characterization of the singular value decomposition, we find

$$(5.21) \quad \sigma_{\min}(\mathbf{H}^* \mathbf{Q}) = \min_{\mathbf{x} \in \mathbb{R}^k} \frac{\|\mathbf{H}^* \mathbf{Q} \mathbf{x}\|^2}{\|\mathbf{x}\|^2} = \min_{\mathbf{x} \in Q_k} \frac{\|\mathbf{H}^* \mathbf{x}\|^2}{\|\mathbf{x}\|^2} = \min_{\mathbf{x} \in Q_k} \frac{\|\mathbf{P}_{H_k} \mathbf{x}\|^2}{\|\mathbf{x}\|^2}$$

and likewise

$$(5.22) \quad \sigma_{\min}(\mathbf{H}^* \mathbf{Q}) = \min_{\mathbf{x} \in \mathbb{R}^k} \frac{\|\mathbf{Q}^* \mathbf{H} \mathbf{x}\|^2}{\|\mathbf{x}\|^2} = \min_{\mathbf{x} \in H_k} \frac{\|\mathbf{Q}^* \mathbf{x}\|^2}{\|\mathbf{x}\|^2} = \min_{\mathbf{x} \in H_k} \frac{\|\mathbf{P}_{Q_k} \mathbf{x}\|^2}{\|\mathbf{x}\|^2},$$

so that we must have

$$(5.23) \quad \min_{\mathbf{x} \in Q_k} \frac{\|\mathbf{P}_{H_k} \mathbf{x}\|^2}{\|\mathbf{x}\|^2} = \min_{\mathbf{x} \in H_k} \frac{\|\mathbf{P}_{Q_k} \mathbf{x}\|^2}{\|\mathbf{x}\|^2}.$$

To reduce further, we observe for any $\mathbf{x} \in H_k$ and $\mathbf{y} \in \text{range}[\mathbf{U}] \cap Q_k^\perp$, there is an orthogonality relationship

$$(5.24) \quad \langle \mathbf{x}, \mathbf{y} \rangle = \langle \mathbf{x}, \mathbf{P}_U \mathbf{y} \rangle = \langle \mathbf{P}_U \mathbf{x}, \mathbf{y} \rangle = 0,$$

because \mathbf{y} lies in the range of \mathbf{U} and orthogonal to $Q_k = \mathbf{P}_U H_k$. It follows

$$(5.25) \quad \min_{\mathbf{x} \in H_k} \frac{\|\mathbf{P}_{Q_k} \mathbf{x}\|^2}{\|\mathbf{x}\|^2} = \min_{\mathbf{x} \in H_k} \frac{\|(\mathbf{P}_{Q_k} + \mathbf{P}_U - \mathbf{P}_{Q_k}) \mathbf{x}\|^2}{\|\mathbf{x}\|^2} = \min_{\mathbf{x} \in H_k} \frac{\|\mathbf{P}_U \mathbf{x}\|^2}{\|\mathbf{x}\|^2}.$$

Combining the calculations above, we obtain the variational inequality

$$(5.26) \quad \min_{\mathbf{x} \in S} \frac{\mathbf{x}^* \mathbf{P}_J \mathbf{x}}{\|\mathbf{x}\|^2} \geq \min_{\mathbf{x} \in H_k} \frac{\|\mathbf{P}_U \mathbf{x}\|^2}{\|\mathbf{x}\|^2} = \cos^2 \theta.$$

Finishing the proof, for any $\mathbf{x} \in S$, we can decompose

$$(5.27) \quad \mathbf{x} = \mathbf{P}_J \mathbf{x} + \mathbf{P}_{H_k^\perp} \mathbf{x},$$

where we have used the fact that J , J' and H_k^\perp form an orthogonal decomposition of \mathbb{R}^n , and \mathbf{x} must be orthogonal to J' (because of (5.15)). Combining (5.27) with (5.26), we find

$$(5.28) \quad \min_{\mathbf{x} \in S} \frac{\mathbf{x}^* \mathbf{P}_J \mathbf{x}}{\|\mathbf{x}\|^2} \geq \cos^2 \theta, \quad \max_{\mathbf{x} \in S} \frac{\mathbf{x}^* \mathbf{P}_{H_k^\perp} \mathbf{x}}{\|\mathbf{x}\|^2} \leq \sin^2 \theta.$$

Additionally, for any $i \geq 0$, we observe that $\mathbf{P}_J \mathbf{A}^i|_J$ has spectrum contained in $[\lambda_j^i, \infty)$ and $\mathbf{P}_{H_k^\perp} \mathbf{A}^i|_{H_k^\perp}$ has spectrum contained in $[-|\lambda_{\beta(k+1)}|^i, |\lambda_{\beta(k+1)}|^i]$, so that

$$(5.29) \quad \min_{\mathbf{x} \in \mathbb{R}^n} \frac{\mathbf{x}^* \mathbf{P}_J \mathbf{A}^i \mathbf{P}_J \mathbf{x}}{\mathbf{x}^* \mathbf{P}_J \mathbf{x}} \geq \lambda_j^i, \quad \max_{\mathbf{x} \in \mathbb{R}^n} \left| \frac{\mathbf{x}^* \mathbf{P}_{H_k^\perp} \mathbf{A}^i \mathbf{P}_{H_k^\perp} \mathbf{x}}{\mathbf{x}^* \mathbf{P}_{H_k^\perp} \mathbf{x}} \right| \leq |\lambda_{\beta(k+1)}|^i.$$

Lastly, using (5.27), (5.28), and (5.29), we are able to conclude

$$(5.30) \quad \min_{\mathbf{x} \in S} \frac{\mathbf{x}^* \mathbf{A}^{i+1} \mathbf{x}}{\mathbf{x}^* \mathbf{A}^i \mathbf{x}}$$

$$(5.31) \quad = \min_{\mathbf{x} \in S} \frac{\mathbf{x}^* \mathbf{P}_J \mathbf{A}^{(i+1)} \mathbf{P}_J \mathbf{x} + \mathbf{x}^* \mathbf{P}_{H_k^\perp} \mathbf{A}^{i+1} \mathbf{P}_{H_k^\perp} \mathbf{x}}{\mathbf{x}^* \mathbf{P}_J \mathbf{A}^i \mathbf{P}_J \mathbf{x} + \mathbf{x}^* \mathbf{P}_{H_k^\perp} \mathbf{A}^i \mathbf{P}_{H_k^\perp} \mathbf{x}}$$

$$(5.32) \quad \geq \frac{\lambda_j^{i+1} \cos^2 \theta - \sin^2 \theta |\lambda_{\beta(k+1)}|^{i+1}}{\lambda_j^i \cos^2 \theta + \sin^2 \theta |\lambda_{\beta(k+1)}|^i}$$

$$(5.33) \quad = \frac{1 - \tan^2 \theta R^{i+1}}{1 + \tan^2 \theta R^i} \lambda_{\beta(j)}.$$

□

The error bound (5.11) is a sharper version of the error bound presented by G. W. Stewart [56], and it has the advantage of showing clearly how the error depends on the range of starting matrix \mathbf{U} : the error is substantially reduced if the $\text{range}[\mathbf{U}]$ lies close to an appropriate subspace of eigenvectors (i.e., $\tan \theta$ is small). The proof presented here is also shorter and more direct than the proof by Stewart, taking advantage of modern strategies for manipulating the min-max principle that were originally introduced by A. Knyazev in [31].

Proposition 5.1 is flexible. We can extend this proposition to the case of negative eigenvalues by considering $-\mathbf{A}$ instead of \mathbf{A} , and can likewise obtain error bounds for the eigenvalue magnitudes. As another alternative, we can simplify the error bound

(5.11) slightly (at the cost of reducing some of the sharpness) by taking ratios and manipulating terms to yield

$$(5.34) \quad 0 \leq \frac{\lambda_j - \Lambda_{jj}^{(i)}}{\lambda_j} \leq 2 \tan^2 \theta \left| \frac{\lambda_{\beta(k+1)}}{\lambda_j} \right|^i, \quad 1 \leq j \leq k, \quad i \geq 0,$$

which emphasizes how the relative eigenvalue error decays exponentially fast, in proportion to the relative eigenvalue gap $|\lambda_{\beta(k+1)}/\lambda_j|^i$. As a consequence of (5.34), we anticipate that deterministic subspace iteration is most successful at estimating the first few eigenvalues and the accuracy degrades for eigenvalues with higher indices.

In Proposition 5.1, we have analyzed the eigenvalue estimates based on solving (2.3), yet our analysis also extends to the more standard eigenvalue estimates based on solving the symmetric eigenvalue problem (2.2). In this case, the variational characterization of the eigenvalues becomes

$$(5.35) \quad \Lambda_{jj}^{(i)} = \max_{\substack{S \subseteq \text{range}[\mathbf{U}] \\ \dim[S]=j}} \min_{\mathbf{x} \in S} \frac{\mathbf{x}^* \mathbf{A}^{2i+1} \mathbf{x}}{\mathbf{x}^* \mathbf{A}^{2i} \mathbf{x}}, \quad 1 \leq j \leq k, \quad i \geq 0,$$

which differs slightly from (5.4) because the matrices \mathbf{A}^i and \mathbf{A}^{i+1} are replaced by the higher powers \mathbf{A}^{2i} and \mathbf{A}^{2i+1} . Consequently, the rate of convergence is twice as fast using the estimator (2.2), i.e.,

$$(5.36) \quad 0 \leq \frac{\lambda_j - \Lambda_{jj}^{(i)}}{\lambda_j} \leq 2 \tan^2 \theta \left| \frac{\lambda_{\beta(k+1)}}{\lambda_j} \right|^{2i}, \quad 1 \leq j \leq k.$$

Yet despite this faster rate of convergence, we prefer not to use (2.2) as the foundation for our randomized subspace iteration. The reason is that empirically we find *randomized* subspace iteration produces much more accurate estimates using (2.3), due to substantial bias resulting from the quadratic term $\mathbf{X}^{(i)*} \mathbf{A} \mathbf{X}^{(i)}$ on the left-hand side of (2.2).

5.2. Analysis of stochastic compression. In our randomized version of subspace iteration, we enforce sparsity in the iterates by applying stochastic compression. Stochastic compression is a random operation that replaces a vector \mathbf{x} with a random vector $\Phi(\mathbf{x})$ that is unbiased, i.e., $\mathbb{E}\Phi(\mathbf{x}) = \mathbf{x}$ and satisfies a sparsity threshold $\|\Phi(\mathbf{x})\|_0 \leq m$.

Because stochastic compression contributes variance to eigenvalue estimates, a major goal of algorithmic design is to ensure the perturbations $\mathbf{x} - \Phi(\mathbf{x})$ are as small as possible in an appropriate norm. In this work we explicitly optimize Φ to minimize the expected square residual $\mathbb{E}\|\mathbf{x} - \Phi(\mathbf{x})\|_2^2$.

PROPOSITION 5.2. *For any $\mathbf{x} \in \mathbb{R}^n$, the solution to the minimization problem*

$$(5.37) \quad \min_{\Phi(\mathbf{x})} \left\{ \mathbb{E}\|\mathbf{x} - \Phi(\mathbf{x})\|_2^2 : \|\Phi(\mathbf{x})\|_0 \leq m, \mathbb{E}\Phi(\mathbf{x}) = \mathbf{x} \right\},$$

must satisfy the following properties:

1. *The largest-magnitude entries $|\mathbf{x}_{\alpha(1)}| \geq \dots \geq |\mathbf{x}_{\alpha(k)}|$ are preserved exactly, i.e., $\Phi(\mathbf{x})_{\alpha(i)} = \mathbf{x}_{\alpha(i)}$.*
2. *The smallest-magnitude entries $|\mathbf{x}_{\alpha(k+1)}| \geq \dots \geq |\mathbf{x}_{\alpha(n)}|$ are randomly perturbed, i.e., $\Phi(\mathbf{x})_{\alpha(i)} = \mathbf{x}_{\alpha(i)}/\mathbf{p}_{\alpha(i)}$ with probability $\mathbf{p}_{\alpha(i)}$ and $\Phi(\mathbf{x})_{\alpha(i)} = 0$ otherwise, where*

$$(5.38) \quad \mathbf{p}_{\alpha(i)} = (m - k) |\mathbf{x}_{\alpha(i)}| / \sum_{j=k+1}^n |\mathbf{x}_{\alpha(j)}|.$$

3. The number k is as small as possible while ensuring $\mathbf{p}_{\alpha(i)} < 1$ for $i \geq k + 1$.

Proof. For any random vector $\Phi(\mathbf{x})$, we introduce the associated vector $\Psi \in \{0, 1\}^n$ with entries

$$(5.39) \quad \Psi_i = \mathbb{1} \{ \Phi(\mathbf{x})_i \neq 0 \}, \quad 1 \leq i \leq n.$$

Thus, Ψ_i is the indicator function on the event $\Phi(\mathbf{x})_i \neq 0$, that is, its value is 1 if this event occurs and its value is 0 otherwise.

The random vector Ψ is useful for the optimization of $\Phi(\mathbf{x})$. Indeed, using the unbiasedness condition $\mathbf{E}\Phi(\mathbf{x})_i = \mathbf{x}_i$, we can explicitly compute the conditional expectations

$$(5.40) \quad \mathbf{E}[\Phi(\mathbf{x})_i | \Psi_i] = \frac{\Psi_i}{\mathbf{E}\Psi_i} \mathbf{x}_i, \quad 1 \leq i \leq n.$$

Hence, the square error $\mathbf{E} \|\mathbf{x} - \Phi(\mathbf{x})\|_2^2$ can be decomposed as

$$(5.41) \quad \sum_{i=1}^n \mathbf{E} |\mathbf{x}_i - \Phi(\mathbf{x})_i|^2$$

$$(5.42) \quad = \sum_{i=1}^n \mathbf{E} |\mathbf{x}_i - \mathbf{E}[\Phi(\mathbf{x})_i | \Psi_i]|^2 + \sum_{i=1}^n \mathbf{E} |\mathbf{E}[\Phi(\mathbf{x})_i | \Psi_i] - \Phi(\mathbf{x})_i|^2$$

$$(5.43) \quad = \sum_{i=1}^n \mathbf{x}_i^2 \left(\frac{1}{\mathbf{E}\Psi_i} - 1 \right) + \sum_{i=1}^n \mathbf{E} \left| \frac{\Psi_i}{\mathbf{E}\Psi_i} \mathbf{x}_i - \Phi(\mathbf{x})_i \right|^2.$$

We can minimize (5.43) by taking $\Phi(\mathbf{x})_i = \mathbf{x}_i \Psi_i / \mathbf{E}\Psi_i$ for $1 \leq i \leq n$, and choosing $\mathbf{E}\Psi \in [0, 1]^n$ to solve

$$(5.44) \quad \min_{\mathbf{E}\Psi \in [0, 1]^n} \left\{ \sum_{i=1}^n \mathbf{x}_i^2 \left(\frac{1}{\mathbf{E}\Psi_i} - 1 \right) : \|\mathbf{E}\Psi\|_1 \leq m \right\},$$

which is a convex optimization problem with linear inequality constraints.

To solve the reduced optimization problem (5.44), we let $\alpha(1), \dots, \alpha(n)$ be a permutation that reorders the elements of \mathbf{x} from largest to smallest magnitude, i.e., $|\mathbf{x}_{\alpha(1)}| \geq \dots \geq |\mathbf{x}_{\alpha(n)}|$, and we introduce the Lagrangian function

$$(5.45) \quad \mathcal{L}(\mathbf{E}\Psi, \eta, \boldsymbol{\lambda}) = \sum_{i=1}^n \mathbf{x}_i^2 \left(\frac{1}{\mathbf{E}\Psi_i} - 1 \right) + \eta (\|\mathbf{E}\Psi\|_1 - m) + \sum_{i=1}^n \lambda_i (\mathbf{E}\Psi_i - 1).$$

Then, the solution to (5.44) must satisfy the gradient condition $\nabla_{\mathbf{E}\Psi} \mathcal{L}(\mathbf{E}\Psi, \eta, \boldsymbol{\lambda}) = 0$, which leads to

$$(5.46) \quad \mathbf{E}\Psi_i = \frac{|\mathbf{x}_i|}{(\eta + \lambda_i)^{1/2}}, \quad 1 \leq i \leq n,$$

as well as the complementarity condition $\lambda_i (\mathbf{E}\Psi_i - 1) = 0$, which leads to

$$(5.47) \quad \mathbf{E}\Psi_i = \frac{|\mathbf{x}_i|}{\eta^{1/2}} \quad \text{or} \quad \mathbf{E}\Psi_i = 1, \quad 1 \leq i \leq n.$$

Additionally, we observe that the objective function (5.44) is minimized by setting $E\Psi_i = 1$ only for the k largest values of \mathbf{x}_i^2 , where $0 \leq k \leq m$ is an unknown parameter. In summary, the largest-magnitude entries satisfy

$$(5.48) \quad E\Psi_{\alpha(i)} = 1, \quad 1 \leq i \leq k,$$

and the smallest-magnitude entries satisfy

$$(5.49) \quad E\Psi_{\alpha(i)} = \frac{(m-k) |\mathbf{x}_{\alpha(i)}|}{\sum_{j=k+1}^n |\mathbf{x}_{\alpha(j)}|}, \quad k+1 \leq i \leq n.$$

The value of the objective function (5.44) becomes

$$(5.50) \quad \sum_{i=k+1}^n \mathbf{x}_{\alpha(i)}^2 \left(\frac{\sum_{j=k+1}^n |\mathbf{x}_{\alpha(j)}|}{(m-k) |\mathbf{x}_{\alpha(i)}|} - 1 \right),$$

and a direct computation reveals (5.50) to be nondecreasing in k , whence k should be taken as small as possible while ensuring that $E\Psi_i \leq 1$ for all $1 \leq i \leq n$. \square

From Proposition 5.2, we find that pivotal compression is optimal in terms of minimizing the expected square residual $E \|\mathbf{x} - \Phi(\mathbf{x})\|_2^2$. In contrast, simpler approaches to stochastic compression based on sampling uniformly at random would introduce larger errors. Indeed, in our empirical tests (Appendix A.3), we find pivotal resampling to be the most effective known compression scheme, outperforming the systematic compression scheme used in [34] and in [22] where systematic compression was shown to substantially outperform alternatives based on, for example, multinomial resampling.

5.3. Analysis of randomized subspace iteration. We do not attempt to derive explicit *a priori* error bounds for randomized subspace iteration (Algorithm 4.1). However, by identifying that the iterates $\mathbf{X}^{(0)}, \mathbf{X}^{(1)}, \mathbf{X}^{(2)}, \dots$ from randomized subspace iteration are embedded in a Markov chain, we can obtain an implicit description of the method's behavior and we can estimate the variance of eigenvalue estimates *a posteriori*. Recalling the definition $\mathbf{Y}^{(i)} = \mathbf{A}\Phi(\mathbf{X}^{(i)})$, our approach is to introduce the block matrix

$$(5.51) \quad \mathbf{\Gamma}^{(i)} = \begin{bmatrix} \mathbf{X}^{(\Delta i)} & \mathbf{Y}^{(\Delta i)} & \mathbf{X}^{(\Delta i+1)} & \mathbf{Y}^{(\Delta i+1)} & \dots \\ & & & & \\ & & \mathbf{X}^{(\Delta(i+1)-1)} & \mathbf{Y}^{(\Delta(i+1)-1)} & \mathbf{N}^{(\Delta(i+1)-1)} \end{bmatrix},$$

where Δ is the orthogonalization interval ($\Delta = 1000$ in our experiments) and observe that the sequence $\mathbf{\Gamma}^{(0)}, \mathbf{\Gamma}^{(1)}, \dots$ satisfies

$$(5.52) \quad \text{Law} \left(\mathbf{\Gamma}^{(i)} | \mathbf{\Gamma}^{(i-1)}, \dots, \mathbf{\Gamma}^{(0)} \right) = \text{Law} \left(\mathbf{\Gamma}^{(i)} | \mathbf{\Gamma}^{(i-1)} \right)$$

and is therefore a Markov chain. Indeed, the sequence $\mathbf{\Gamma}^{(0)}, \mathbf{\Gamma}^{(1)} \dots$ satisfies an even stronger conditional independence property than (5.52), because the distribution of $\mathbf{\Gamma}^{(i)}$ is determined entirely from the last three blocks of $\mathbf{\Gamma}^{(i-1)}$ by applying (4.1) $\Delta - 1$ times with diagonal normalization and then applying (4.1) one final time with orthogonalization as detailed in Algorithm 4.1.

Due to the Markov chain structure, we can apply general results governing the asymptotic behavior of Markov chains, specifically the strong law of large numbers

and Markov chain central limit theorem, which hold under a geometric ergodicity assumption [37, 29]. This asymptotic theory is general to Markov chains, so we do not expect it to lead to any specific *a priori* bounds concerning the accuracy of randomized subspace iteration. However, this theory does lead to qualitative predictions, first that the estimated eigenvalues $\Lambda^{(i_{\max})}$ converge to a deterministic limit as $i \rightarrow \infty$ and second that the variation around this limit is asymptotically Gaussian with a variance that can be calculated *a posteriori* from data.

PROPOSITION 5.3. *Assume the Markov chain $\Gamma^{(0)}, \Gamma^{(1)}, \dots$ is geometrically ergodic with respect to a distribution μ , and the variables*

$$(5.53) \quad \frac{1}{\Delta} \sum_{i=0}^{\Delta-1} \mathbf{U}^* \mathbf{X}^{(i)} \quad \text{and} \quad \frac{1}{\Delta} \sum_{i=0}^{\Delta-1} \mathbf{U}^* \mathbf{Y}^{(i)}$$

are square-integrable with respect to μ , having expectations $\mathbf{E}^{(\infty)}$ and $\mathbf{F}^{(\infty)}$ respectively. Then, the estimated eigenvalues from randomized subspace iteration converge with probability one

$$(5.54) \quad \lim_{i_{\max} \rightarrow \infty} \Lambda^{(i_{\max})} = \Lambda^{(\infty)},$$

where $\Lambda^{(\infty)}$ is the the solution to the generalized eigenvalue problem

$$(5.55) \quad \mathbf{F}^{(\infty)} \mathbf{W}^{(\infty)} \Lambda^{(\infty)} = \mathbf{E}^{(\infty)} \mathbf{W}^{(\infty)}.$$

Moreover, for any simple eigenvalue $\Lambda_{jj}^{(\infty)}$ with corresponding left eigenvector $\mathbf{z}_j^{(\infty)}$ and right eigenvector $\mathbf{w}_j^{(\infty)}$, the deviations of $\Lambda_{jj}^{(i_{\max})}$ from $\Lambda_{jj}^{(\infty)}$ are asymptotically Gaussian

$$(5.56) \quad \sqrt{i_{\max} - i_{\min}} \left(\Lambda_{jj}^{(i_{\max})} - \Lambda_{jj}^{(\infty)} \right) \rightarrow \mathcal{N}(0, \sigma_j^2),$$

and the asymptotic variance is given by the expression

$$(5.57) \quad \sigma_j^2 = \frac{1}{\Delta} \sum_{i=0}^{\Delta-1} \sum_{k=-\infty}^{\infty} \text{Cov} \left[f_j^{(i)}, f_j^{(k)} \right],$$

where $f_j^{(i)}$ is the scalar-valued time series

$$(5.58) \quad f_j^{(i)} = \mathbf{z}_j^{(\infty)} \left(\mathbf{U}^* \mathbf{X}^{(i)} - \Lambda_{jj}^{(\infty)} \mathbf{U}^* \mathbf{Y}^{(i)} \right) \mathbf{w}_j^{(\infty)}.$$

Proof. Using the geometric ergodicity assumption and strong law of large numbers for Markov chains [37], we confirm that almost surely

$$(5.59) \quad \mathbf{E}^{(i_{\max})} = \frac{1}{i_{\max} - i_{\min}} \sum_{i=i_{\min}}^{i_{\max}-1} \mathbf{U}^* \mathbf{X}^{(i)} \rightarrow \mathbf{E}^{(\infty)}$$

and

$$(5.60) \quad \mathbf{F}^{(i_{\max})} = \frac{1}{i_{\max} - i_{\min}} \sum_{i=i_{\min}}^{i_{\max}-1} \mathbf{U}^* \mathbf{Y}^{(i)} \rightarrow \mathbf{F}^{(\infty)}$$

as $i_{\max} \rightarrow \infty$. Moreover, (5.59), (5.60), and the continuity of eigenvalues [58] in the generalized eigenvalue problem together imply that $\mathbf{\Lambda}^{(i_{\max})} \rightarrow \mathbf{\Lambda}^{(i_{\infty})}$ almost surely as $i_{\max} \rightarrow \infty$, confirming equation (5.54).

For the asymptotic Gaussianity result, we use the first-order perturbation theory for simple eigenvalues in the generalized eigenvalue problem (see e.g., [58, 21]), which reveals that

$$(5.61) \quad \mathbf{\Lambda}_{jj}^{(i)} - \mathbf{\Lambda}_{jj}^{(\infty)} = \mathbf{z}_j^{(\infty)} \left(\mathbf{E}^{(i)} - \mathbf{\Lambda}_{jj}^{(\infty)} \mathbf{F}^{(i)} \right) \mathbf{w}_j^{(\infty)} + \mathcal{O} \left(\mathbf{E}^{(i)} - \mathbf{E}^{(\infty)} \right)^2 + \mathcal{O} \left(\mathbf{F}^{(i)} - \mathbf{F}^{(\infty)} \right)^2$$

as $i_{\max} \rightarrow \infty$. Additionally, by the Markov chain central limit theorem [29], we can confirm that quantities $\mathbf{E}^{(i)} - \mathbf{E}^{(\infty)}$ and $\mathbf{F}^{(i)} - \mathbf{F}^{(\infty)}$ are asymptotically $\mathcal{O}_P(\sqrt{i_{\max}})$ as $i_{\max} \rightarrow \infty$ and also

$$(5.62) \quad \sqrt{i_{\max} - i_{\min}} \mathbf{z}_j^{(\infty)} \left(\mathbf{E}^{(i)} - \mathbf{\Lambda}_{jj}^{(\infty)} \mathbf{F}^{(i)} \right) \mathbf{w}_j^{(\infty)} \xrightarrow{\mathcal{D}} \mathcal{N}(0, \sigma_j^2),$$

where the asymptotic variance σ_j^2 is defined in (5.57). Using Slutsky's lemma [25] together with (5.61) and (5.62), we verify the main result that

$$(5.63) \quad \sqrt{i_{\max} - i_{\min}} \left(\mathbf{\Lambda}_{jj}^{(i_{\max})} - \mathbf{\Lambda}_{jj}^{(\infty)} \right) \rightarrow \mathcal{N}(0, \sigma_j^2). \quad \square$$

As a consequence of Proposition 5.3, the quality of each eigenvalue estimate $\mathbf{\Lambda}_{jj}^{(i_{\max})}$ is mainly determined by the *standard error* and the *asymptotic bias*. The standard error is the stochastic variability of $\mathbf{\Lambda}_{jj}^{(i_{\max})}$ after a certain number of iterations, as defined by

$$(5.64) \quad \sigma_j^{(i_{\max})} = \text{Var}[\mathbf{\Lambda}_{jj}^{(i_{\max})}]^{1/2}.$$

The asymptotic bias is the absolute difference between the estimate after infinitely many iterations and the exact eigenvalue, as defined by

$$(5.65) \quad b_j = |\lim_{i_{\max} \rightarrow \infty} \mathbf{\Lambda}_{jj}^{(i_{\max})} - \lambda_j|.$$

Empirically, we find that increasing m in compression operations decreases both the standard error $\sigma_j^{(i_{\max})}$ and the asymptotic bias b_j . In contrast, averaging over more iterations (i.e. increasing i_{\max}) decreases only the standard error $\sigma_j^{(i_{\max})}$.

Lastly, by taking advantage of the explicit expression (5.58), we can compute the standard error in each eigenvalue estimate as follows. We let \mathbf{w}_j and \mathbf{z}_j denote the left and right generalized eigenvectors corresponding to the eigenvalue $\mathbf{\Lambda}_{jj}^{(i_{\max})}$ in eq 4.4 and define the scalar-valued time series

$$(5.66) \quad f_j^{(i)} = \mathbf{z}_j^* \left(\mathbf{U}^* \mathbf{Y}^{(i)} - \mathbf{\Lambda}_{jj}^{(i_{\max})} \mathbf{U}^* \mathbf{X}^{(i)} \right) \mathbf{w}_j.$$

Then, from (5.57) the variance in $\mathbf{\Lambda}_{jj}^{(i_{\max})}$ is well-approximated by

$$(5.67) \quad \text{Var}[\mathbf{\Lambda}_{jj}^{(i_{\max})}] \approx \frac{1}{(i_{\max} - i_{\min})^2} \sum_{\substack{i_{\min} \leq i, k \leq i_{\max} - 1 \\ |i - k| \leq \tau}} \text{Cov} \left[f_j^{(i)}, f_j^{(k)} \right],$$

where the truncation threshold τ is chosen large enough that the correlations involving $f_j^{(i)}$ and $f_j^{(k)}$ are negligibly small for any $|i - k| > \tau$ [52]. These *a posteriori* variance formulas enable the explicit calculation of the standard error terms $\sigma_j^{(i_{\max})}$, which can be very useful for measuring and reducing stochastic errors in eigenvalue estimates.

TABLE 1

Parameters used in numerical calculations of FCI eigenvalues. N and M denote the number of active electrons and orbitals, respectively, for each system, as determined by the choice of single-electron basis. n_{FCI} is the dimension of the block of the FCI matrix containing the lowest-energy eigenvalue.

System	Nuclear separation	Single-electron basis	(N, M)	$n_{\text{FCI}}/10^6$
Ne	-	aug-cc-pVDZ	(8, 22)	6.69
equilibrium C_2	1.27273 Å	cc-pVDZ	(8, 26)	27.9
stretched C_2	2.22254 Å	cc-pVDZ	(8, 26)	27.9

6. Numerical experiments. We assess the performance of our method by applying it to the full configuration interaction (FCI) problem from quantum chemistry. Quantum chemistry methods like FCI can be applied to predict the properties of molecules (e.g. their atomic geometries, behavior in chemical reactions, or response to stimulation by light). Many practical methods seek to approximate the FCI eigenvalues; these approximations are necessary for reducing the computational cost and enabling the application to larger chemical systems. But these approximate methods are not always systematically improvable, and they can fail in some important cases, so FCI-quality results are needed to benchmark their accuracy. In most cases, estimating eigenvalues to within $1 \text{ m}E_{\text{h}}$ is necessary for chemical accuracy [9], where $\text{m}E_{\text{h}}$ denotes the milliHartree unit of energy.

The FCI Hamiltonian matrix \mathbf{H} encodes the physics of interacting electrons in a field of fixed nuclei. It is expressed in a basis of Slater determinants, each representing a configuration of N electrons in M single-electron orbitals, here taken to be canonical Hartree-Fock orbitals. Elements of \mathbf{H} are given by the Slater-Condon rules [50, 16], which also determine its sparsity structure; only $\mathcal{O}(N^2 M^2)$ elements per column are nonzero. We subtracted the Hartree-Fock energy from all diagonal elements.

The dimension of \mathbf{H} depends combinatorially on M and N . For many molecules, symmetry can be used to construct a basis in which the Hamiltonian matrix is block diagonal, effectively reducing the dimension. Here, we consider only the spatial (i.e. point-group) symmetry of the nuclei, although other symmetries (e.g. electron spin or angular momentum) could be used to further reduce the dimension. Many randomized methods leverage this block-diagonal structure to estimate multiple eigenvalues, namely by calculating the dominant eigenvalue of each block independently. Here we focus on the more challenging task of estimating multiple eigenvalues within a single block, namely the one containing the lowest-energy eigenvalue.

Table 1 lists the parameters defining the FCI matrix for each molecular system considered here. We used the PySCF software [59] to calculate matrix elements, point-group symmetry labels, and reference eigenvalues to which results are compared. The dimensions of these problems are small enough that their eigenvalues can be obtained by standard deterministic iterative methods. For such small problems, commonly used deterministic methods are often more efficient than the randomized approaches presented here, especially considering the slow convergence of deterministic subspace iteration relative to better-performing schemes like Jacobi-Davidson [17, 51]. Nevertheless, we focus here on these small problems in order to demonstrate the features of our randomized approach and assess its accuracy through comparisons with exact eigenvalues from deterministic methods. Previously, we demonstrated that algorithms based on our randomization approach can enable the calculation of highly accurate es-

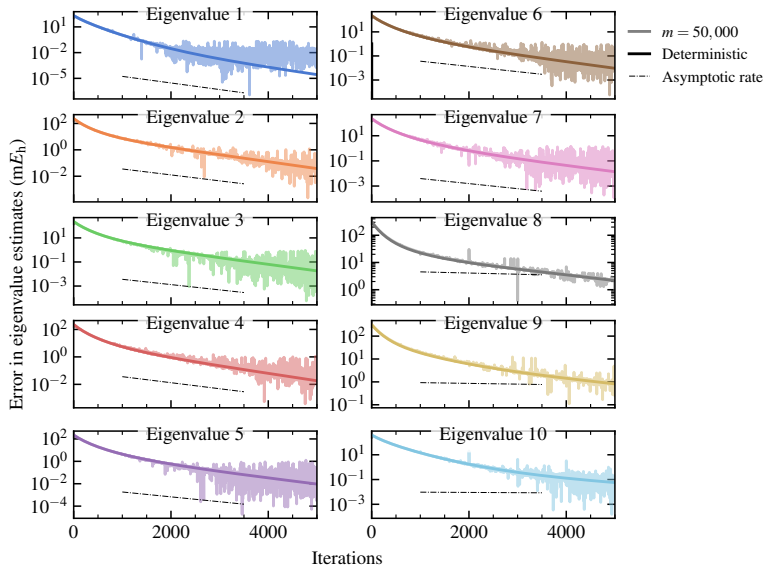


FIG. 1. Errors in eigenvalue estimates (relative to exact) for the Ne atom, obtained by applying deterministic subspace iteration and our randomized subspace iteration with $m = 50,000$ nonzero elements per column. Dash-dotted lines indicate asymptotic convergence rates proportional to the relative eigenvalue gap $|\lambda_{(k+1)}/\lambda_j|^i$ (5.34). Eigenvalues are ordered in energy, with Eigenvalue 1 being the lowest-energy eigenvalue (i.e. the dominant eigenvalue of \mathbf{A}).

timates of the lowest-energy eigenvalue in high-dimensional FCI problems that cannot be solved using conventional methods [23]. Our future work will focus on extending these strategies for the calculation of multiple eigenvalues for very high-dimensional problems.

The lowest-energy eigenvalues of \mathbf{H} are typically of greatest chemical interest, so we apply our algorithm to $\mathbf{A} = \mathbf{I} - \varepsilon\mathbf{H}$ instead of \mathbf{H} itself. The lowest-energy eigenvectors of \mathbf{H} are the dominant eigenvectors of \mathbf{A} for $\varepsilon > 0$ sufficiently small in magnitude. We used $\varepsilon = 10^{-6} \text{ mE}_h^{-1}$ for all systems. Eigenvalues E_j of \mathbf{H} are related to those λ_j of \mathbf{A} as $E_j = \varepsilon^{-1}(1 - \lambda_j)$.

6.1. Comparing deterministic and randomized results for the Ne atom.

In order to provide a qualitative sense of the performance of our randomized scheme, we first present a comparison to the deterministic scheme presented in Section 2. In order to enable as direct a comparison as possible, we do not apply the averaging techniques presented in Section 4 to reduce stochastic fluctuations in our randomized scheme; instead, we present the instantaneous Ritz values obtained by solving (2.3) after each iteration for both schemes. In both cases, orthogonalization was performed at intervals of 1000 iterations. The resulting estimates of the first ten (lowest-energy) eigenvalues of the FCI Hamiltonian matrix \mathbf{H} for the Ne atom in the aug-cc-pVDZ basis are presented in Figure 1. The dimensions of this matrix are approximately 7 million by 7 million. We constructed the matrix \mathbf{U} of eigenvector estimates by diagonalizing \mathbf{H} in a subspace constructed by restricting orbital occupations (i.e. a complete active space consisting of 8 electrons in 10 orbitals), thereby ensuring that \mathbf{U} is sparse. The resulting matrix has approximately 5000 nonzero elements per column.

The slopes of the black dash-dotted lines in Figure 1 indicate the expected as-

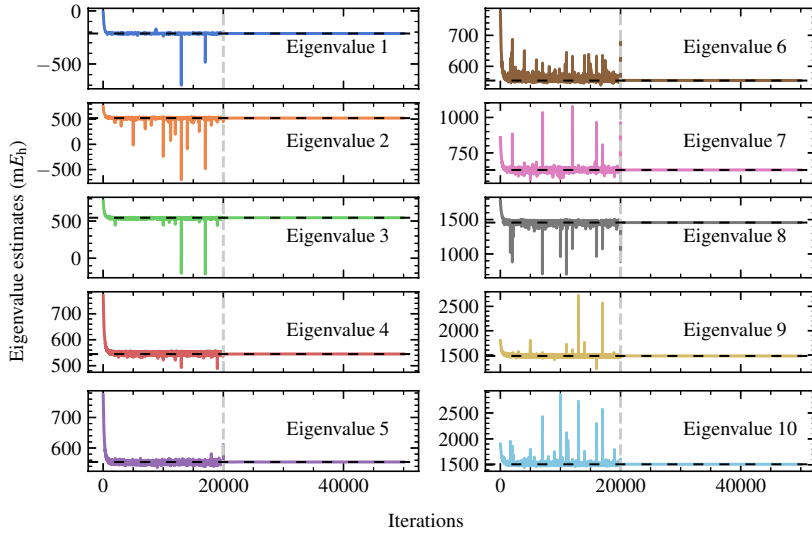


FIG. 2. *Eigenvalue estimates from our randomized subspace iteration. After an initial equilibration period (20,000 iterations), estimates of the first ten FCI eigenvalues for Ne converge to exact eigenvalues (horizontal dashed lines) to within small asymptotic biases when iterate matrices are compressed to $m = 10,000$ nonzero elements per column.*

ymptotic convergence rates for each eigenvalue j , $|\lambda_{(k+1)}/\lambda_j|^i$, as derived in Section 5.1. Estimates of higher-energy eigenvalues appear to converge faster than this rate, possibly indicating that we did not include sufficiently many iterations to reach the asymptotic regime for these eigenvalues. In general, errors in estimates from our randomized scheme follow the same trend as those from the deterministic scheme, but with random fluctuations arising from the compression operations.

6.2. Randomized results for the Ne atom. Fig. 2 presents eigenvalue estimates for this same Ne system, obtained by performing stochastic compressions with $m = 10,000$ nonzero elements per column in each iteration. We show the instantaneous Ritz values for the first 20,000 iterations, after which we begin averaging the $k \times k$ matrices according to (4.4) (i.e. with $i_{\min} = 20,000$). Eigenvalues of the averaged matrices show substantially decreased fluctuations.

Figure 3 shows differences between estimated and exact eigenvalues after 50,000 iterations. With $m = 10,000$, these differences are less than $0.32 mE_h$ and can be attributed to the statistical bias in our method. All standard errors are less than $0.004 mE_h$. Retaining more nonzero elements in compression operations ($m = 50,000$) reduces the asymptotic biases to $< 0.02 mE_h$ and the standard errors to $< 0.0003 mE_h$.

We performed two additional calculations to demonstrate the advantages of the non-standard features of our randomized subspace iteration. First, we replaced the averaging of matrices in (4.4) by averaging of the instantaneous Ritz values $\mathbf{\Lambda}^{(i)}$ (2.3) from each iteration of the same $m = 10,000$ calculation. The resulting eigenvalue estimates have biases as large as $1.48 mE_h$, almost five times larger than their counterparts in Fig. 3. Second, we tested a randomized implementation of a more standard subspace iteration that uses quadratic operations in the orthogonalization and eigenvalue estimation steps. The best estimates from this method with $m = 10,000$ are 43

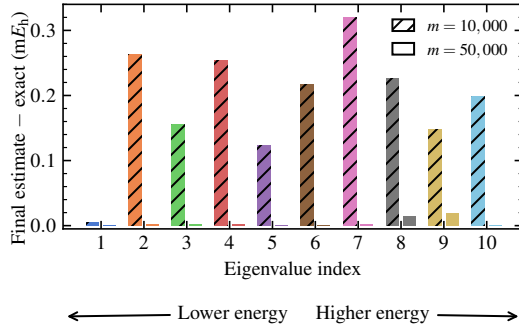


FIG. 3. Errors in final eigenvalue estimates from our randomized subspace iteration after 50,000 iterations. Eigenvalue estimates obtained with $m = 50,000$ exhibit less error than those with $m = 10,000$. All estimates agree with exact eigenvalues to within $0.35 mE_h$.

TABLE 2

Exact eigenvalues (in mE_h) for the equilibrium and stretched C_2 systems, and those calculated by our randomized subspace iteration with $m = 150,000$ or $m = 200,000$, respectively.

equilibrium C_2 ($m = 150,000$)		stretched C_2 ($m = 200,000$)	
Exact	Estimated	Exact	Estimated
-343.40	-343.39	-346.33	-346.32
-264.67	-264.67	-343.50	-343.50
-254.34	-254.34	-322.30	-322.33
-155.40	-155.37	-298.45	-298.45
-104.86	-104.84	-251.24	-251.22
-85.17	-85.15	-250.07	-250.05
-48.91	-48.92	-241.71	-241.72
-19.33	-19.35	-208.54	-208.15
13.64	13.63	-201.02	-199.05
26.44	26.53	-190.49	-190.01

to $161 mE_h$ greater than exact eigenvalues. Details are presented in Appendix C.

6.3. Randomized results for the carbon dimer. In order to evaluate the performance of our randomized subspace iteration for higher-dimensional problems, we apply it to the carbon dimer molecule C_2 , with computational details given in Table 1 and results given in Table 2. Eigenvector estimates \mathbf{U} were constructed from a complete active space calculation with 8 electrons in 9 orbitals. For C_2 at its equilibrium bond length, with iterates compressed to $m = 150,000$ nonzero elements per column, estimates of the ten lowest-energy eigenvalues differ from exact eigenvalues by less than $0.09 mE_h$. Standard errors after 50,000 iterations (choosing $i_{\min} = 20,000$) are less than $4 \times 10^{-5} mE_h$.

The stretched C_2 molecule exhibits stronger electron correlation than the equilibrium C_2 molecule and therefore serves as a more rigorous test for numerical eigenvalue methods in general. Deterministic subspace iteration converges more slowly for stretched C_2 because differences between eigenvalues are smaller (Table 2). Our randomized subspace iteration performs worse for stretched C_2 than for equilibrium C_2 when applied with the same parameters ($m = 150,000$). As the iteration proceeds, random fluctuations in elements of the matrices $\mathbf{U}^* \mathbf{A} \Phi(\mathbf{X}^{(i)})$ and $\mathbf{U}^* \mathbf{X}^{(i)}$ increase,

and ultimately the matrices $\mathbf{U}^* \mathbf{X}^{(i)}$ become singular. This makes it impossible to obtain accurate eigenvalue estimates. In contrast, these fluctuations are significantly reduced when iterates are instead compressed to $m = 200,000$ nonzero elements per column. In this case, eigenvalue estimates differ from exact eigenvalues by less than $2 \text{ m}E_{\text{h}}$, with standard errors less than $9 \times 10^{-5} \text{ m}E_{\text{h}}$. A longer equilibration period ($i_{\text{min}} = 35,000$) was needed to obtain accurate estimates for this problem. These results suggest that each problem may require a minimum value of m to achieve reliable convergence. Others [54, 60] have observed similarly abrupt changes in variance with the amount of sampling in randomized methods for single eigenvalues, but in those cases the variance can in principle be reduced just by averaging over more iterations [23]. In contrast, insufficient sampling in our randomized subspace iteration precludes the estimation of k eigenvalues due to numerical issues encountered when solving (4.4), an issue that cannot be remedied by including more iterations.

7. Discussion. Incorporating random sparsification techniques into iterative linear algebra methods can enable substantial gains in their computational efficiency. Here we present a general technique for extending existing iterative approaches with repeated random sparsification to estimate multiple eigenvalues, and we evaluate its performance in the context of one specific randomization scheme, pivotal compression. We perform numerical experiments on FCI problems from quantum chemistry involving matrices as large as 28 million by 28 million. Even when the number of elements retained in each iteration is less than 1% of the dimension of the matrix, we obtain accurate eigenvalue estimates for three different systems.

Among previous randomized iterative approaches to the multiple eigenvalue problem, ours is perhaps most closely related to several “replica” schemes introduced for quantum applications. Replica schemes use two independent sequences of randomly generated vectors to build subspaces within which the target matrix is subsequently diagonalized [43, 5, 7, 6]. In comparison, our method avoids the high-variance inner products of sparse, random vectors that can hinder replica approaches [5] and results in a stable stochastic iteration that can be averaged to further reduce statistical error. As a notable consequence, and unlike replica methods, our approach is applicable to eigenproblems in continuous space.

A variety of possible improvements could enable application of our method to even larger problems. Several of these have already been developed and tested in the context of the ground-state (i.e. single-eigenvalue) FCI problem [15, 46, 22, 23]. For example, factorizing the matrix \mathbf{A} and employing additional compression operations can further reduce the cost of matrix multiplication in each iteration [22]. Additionally, incorporating random sparsification techniques into other iterative linear algebra methods (e.g. Jacobi-Davidson [17, 51]) may be worth investigating, since their deterministic versions generally converge faster than subspace iteration [8].

Finally, despite their success in high-dimensional applications, explicit *a priori* error bounds for randomized iterative algorithms are lacking. Tackling the complicated correlations between iterates to precisely characterize the dependence of their error on dimension is a pressing and ambitious goal [34].

Appendix A. Compression Algorithms. This section provides further details about the vector compression algorithms introduced in Section 3. We present possible implementations of each of the steps involved in compressing an input vector \mathbf{x} . We then discuss strategies for parallelizing these and other compression schemes. Finally, we present numerical results demonstrating that pivotal compression yields less statistical error than systematic compression, an alternative compression scheme

we have used in our prior work.

A.1. Pivotal Compression. As introduced in Section 3, stochastically compressing a vector \mathbf{x} to m nonzero elements involved three steps, which are summarized in Algorithm A.1: identifying the elements to preserve exactly in the compressed vector, sampling from among the remaining elements, and constructing the compressed vector. Although any unbiased sampling scheme could be used for the stochastic component of this algorithm, we specifically reference pivotal sampling here. Pivotal sampling is described in Algorithm A.2.

Algorithm A.1 Stochastic compression with pivotal sampling

- 1: **Input:** A vector $\mathbf{x} \in \mathbb{R}^n$, a target number of nonzero elements $m \leq n$
 - 2: Set $\mathcal{D} = \emptyset$, $d = 0$.
 - 3: **while** $\max_{i: i \notin \mathcal{D}} |\mathbf{x}_i| \geq \frac{1}{m-d} \sum_{j \notin \mathcal{D}} |\mathbf{x}_j|$ **do**
 - 4: Set $j = \arg \max_{i: i \notin \mathcal{D}} |\mathbf{x}_i|$.
 - 5: Add index j to \mathcal{D} and set $d = d + 1$.
 - 6: **end while**
 - 7: Set $\mathbf{p}_i = 0$ for all $i \in \mathcal{D}$ and set $\mathbf{p}_i = (m - d)|\mathbf{x}_i| / \sum_{j \notin \mathcal{D}} |\mathbf{x}_j|$ for all $i \notin \mathcal{D}$.
 - 8: Apply pivotal sampling (Algorithm A.2) to sample $(m - d)$ elements \mathcal{S} from \mathbf{p} .
 - 9: Set $\Phi(\mathbf{x})_i = \mathbf{x}_i$ for all $i \in \mathcal{D}$, set $\Phi(\mathbf{x})_i = \mathbf{x}_i / \mathbf{p}_i$ for all $i \in \mathcal{S}$, and set $\Phi(\mathbf{x})_i = 0$ for all $i \notin \mathcal{D} \cup \mathcal{S}$.
 - 10: **Return:** Compressed vector $\Phi(\mathbf{x})$
-

Algorithm A.2 Pivotal sampling [13]

- 1: **Input:** A number g of elements to sample, a vector $\mathbf{p} \in \mathbb{R}^n$ of probabilities, with $\sum_i \mathbf{p}_i = g$
 - 2: **Initialization:** Set $\mathcal{S} = \emptyset$, $b = 0$, $l = 0$, $f = 1$
 - 3: **for** $j = 1, 2, \dots, g$ **do**
 - 4: Set $s = \max\{k : b + \sum_{i=f}^k \mathbf{p}_i < 1\}$
 - 5: Randomly select index h from $(l, f, f + 1, f + 2, \dots, s)$ with probabilities proportional to $(b, \mathbf{p}_f, \mathbf{p}_{f+1}, \mathbf{p}_{f+2}, \dots, \mathbf{p}_s)$
 - 6: Set $a = 1 - b - \sum_{i=f}^s \mathbf{p}_i$
 - 7: Set $b = \mathbf{p}_{s+1} - a$
 - 8: With probability $(1 - a(1 - b)^{-1})$, add index h to \mathcal{S} and set $l = s + 1$; otherwise, add index $(s + 1)$ to \mathcal{S} and set $l = h$
 - 9: Set $f = s + 2$
 - 10: **end for**
 - 11: **Return:** Sampled indices \mathcal{S}
-

A.2. Parallelizing vector compression. Here we describe possible strategies for parallelizing each of the two steps involved in pivotal compression of a vector \mathbf{x} . We assume that elements of \mathbf{x} are distributed among n_{procs} parallel processes, not necessarily uniformly, in arbitrary order.

Algorithm A.1 describes a serial implementation of the first step, namely identifying the largest-magnitude elements in \mathbf{x} and determining the number d to preserve exactly. This procedure can be parallelized by noting that elements of \mathbf{x} need not be considered in strict order of decreasing magnitude. We provide pseudocode for this alternative approach in Algorithm A.3, and a complete parallel implementation

is included in the open-source FRIES software on GitHub [1]. The resulting set of deterministic indices $\mathcal{D} = \mathcal{D}^{(1)} \cup \mathcal{D}^{(2)} \cup \dots \cup \mathcal{D}^{(n_{\text{procs}})}$, containing a total of d indices, still satisfies the criteria in (3.2) and (3.1).

Algorithm A.3 Parallel selection of elements for exact preservation

```

1: Input: Vector  $\mathbf{x}^{(j)}$  on each process  $j$  containing elements of the vector to be
   compressed, target number  $m$  nonzero elements across all processes
2: Set  $d = 0$ ,  $\mathcal{D}^{(j)} = \emptyset$  for all  $j$ . ▷ Deterministic indices
3: for  $j = 1, 2, \dots, n_{\text{procs}}$  do ▷ In parallel
4:   Set  $w^{(j)} = \sum_i |\mathbf{x}_i^{(j)}|$ .
5: end for
6: Communicate values of  $w^{(j)}$  among all processes.
7: for  $j = 1, 2, \dots, n_{\text{procs}}$  do ▷ In parallel
8:   Set  $a^{(j)} = 0$ .
9:   while  $\max_{i: i \notin \mathcal{D}} |\mathbf{x}_i^{(j)}| \geq \frac{1}{(m-d-a^{(j)})} \sum_{l=1}^{n_{\text{procs}}} w^{(l)}$  do
10:    Set  $l = \arg \max_{i: i \notin \mathcal{D}^{(j)}} |\mathbf{x}_i^{(j)}|$ 
11:    Add index  $l$  to  $\mathcal{D}^{(j)}$  and set  $a^{(j)} = a^{(j)} + 1$ .
12:    Set  $w^{(j)} = w^{(j)} - |\mathbf{x}_l^{(j)}|$ .
13:   end while
14: end for
15: Set  $d = d + \sum_{j=1}^{n_{\text{procs}}} a^{(j)}$ .
16: if  $\max_j a^{(j)} > 0$  then
17:   Goto line 6.
18: end if
19: Return: Deterministic indices  $\mathcal{D}^{(j)}$  for each process

```

Next we describe an approach to parallelizing the second sampling step in vector compression. The vector \mathbf{p} of probabilities (3.3) is divided into vectors $\mathbf{q}^{(j)}$ containing the elements of the vector on a particular process j . The first step of this parallel approach involves deciding how many elements to sample from the vector of probabilities on each process. The number \mathbf{g}_j of samples assigned to each process is a random number satisfying

$$(A.1) \quad \mathbb{E}[\mathbf{g}_j] = (m - d) \frac{\|\mathbf{q}^{(j)}\|_1}{\|\mathbf{p}\|_1},$$

with the additional constraint $\sum_j \mathbf{g}_j = m - d$. The fact that processes with more of the probability mass are assigned more samples, on average, is one feature that ensures the low variance of this parallel compression technique. We construct \mathbf{g} by sampling $(m - d - \sum_j \lfloor \mathbb{E}[\mathbf{g}_j] \rfloor)$ elements from the vector \mathbf{t} of probabilities, with elements

$$(A.2) \quad \mathbf{t}_j = \mathbb{E}[\mathbf{g}_j] - \lfloor \mathbb{E}[\mathbf{g}_j] \rfloor$$

by using pivotal sampling (Algorithm A.2). Denoting the sampled indices as \mathcal{S}' , elements of \mathbf{g} are given as

$$(A.3) \quad \mathbf{g}_j = \begin{cases} \lfloor \mathbb{E}[\mathbf{g}_j] \rfloor + 1, & j \in \mathcal{S}' \\ \lfloor \mathbb{E}[\mathbf{g}_j] \rfloor, & j \notin \mathcal{S}' \end{cases}$$

This operation can be performed efficiently without parallelization, assuming that the dimension of \mathbf{t} (i.e. the number of parallel processes) is small.

Algorithm A.4 Parallel sampling of vector elements

```

1: Input: Vector  $\mathbf{q}^{(j)}$  containing selection probabilities for elements on each process
    $j$ , total number  $g$  of elements to sample from all processes
2: Set  $c = g$ 
3: for  $j = 1, 2, \dots, n_{\text{procs}}$  do  $\triangleright n_{\text{procs}}$  is the number of processes
4:   Set  $\mathbf{a}_j = g \|\mathbf{q}^{(j)}\|_1 (\sum_i \|\mathbf{q}^{(i)}\|_1)^{-1}$ 
5:   Set  $\mathbf{t}_j = \mathbf{a}_j - \lfloor \mathbf{a}_j \rfloor$ 
6:   Set  $\mathbf{g}_j = \lfloor \mathbf{a}_j \rfloor$ 
7:   Set  $c = c - \mathbf{g}_j$ 
8: end for
9: Sample  $c$  elements  $\mathcal{S}'$  from  $\mathbf{t}$  by pivotal sampling (Algorithm A.2)
10: Add 1 to  $\mathbf{g}_j$  for each  $j \in \mathcal{S}$ 
11: for  $j = 1, 2, \dots, n_{\text{procs}}$  do  $\triangleright$  In parallel
12:   Set  $\mathbf{s}_j = \sum_i \mathbf{q}_i^{(j)}$ 
13:   if  $\mathbf{g}_j > \mathbf{a}_j$  then
14:     for  $i = 1, 2, \dots$  do
15:        $\mathbf{y}_i^{(j)} = \min \{1, \mathbf{q}_i^{(j)} / \mathbf{t}_j\}$ 
16:       Set  $\mathbf{s}_j = \mathbf{s}_j + \mathbf{y}_i^{(j)} - \mathbf{q}_i^{(j)}$ 
17:       Set  $\mathbf{q}_i^{(j)} = \mathbf{y}_i^{(j)}$ 
18:       if  $\mathbf{s}_j \geq \mathbf{g}_j$  then
19:         Set  $\mathbf{q}_i^{(j)} = \mathbf{y}_i^{(j)} + \mathbf{g}_j - \mathbf{s}_j$ 
20:         Terminate for loop
21:       end if
22:     end for
23:   else
24:     for  $i = 1, 2, \dots$  do
25:        $\mathbf{y}_i^{(j)} = \max \{0, (\mathbf{q}_i^{(j)} - \mathbf{t}_j) / (1 - \mathbf{t}_j)\}$ 
26:       Set  $\mathbf{s}_j = \mathbf{s}_j + \mathbf{y}_i^{(j)} - \mathbf{q}_i^{(j)}$ 
27:       Set  $\mathbf{q}_i^{(j)} = \mathbf{y}_i^{(j)}$ 
28:       if  $\mathbf{s}_j \leq \mathbf{g}_j$  then
29:         Set  $\mathbf{q}_i^{(j)} = \mathbf{y}_i^{(j)} + \mathbf{g}_j - \mathbf{s}_j$ 
30:         Terminate for loop
31:       end if
32:     end for
33:   end if
34: end for
35: Sample  $\mathbf{g}_j$  elements from  $\mathbf{q}^{(j)}$  on each process  $j$  by pivotal sampling (Algorithm
   A.2, in parallel)

```

Next, the probabilities on each process j must be adjusted to ensure that their sum is \mathbf{g}_j . This adjustment is performed differently depending on whether $\mathbf{g}_j > \mathbb{E}[\mathbf{g}_j]$ or $\mathbf{g}_j < \mathbb{E}[\mathbf{g}_j]$. No adjustment is needed if $\mathbf{g}_j = \mathbb{E}[\mathbf{g}_j]$, i.e. if $\mathbb{E}[\mathbf{g}_j]$ is integer-valued. We define the vectors $\mathbf{y}^{(j)}$, with elements

$$(A.4) \quad \mathbf{y}_i^{(j)} = \begin{cases} \min \{1, \mathbf{q}_i^{(j)} / \mathbf{t}_j\} & \mathbf{g}_j > \mathbb{E}[\mathbf{g}_j] \\ \max \{0, (\mathbf{q}_i^{(j)} - \mathbf{t}_j) / (1 - \mathbf{t}_j)\} & \mathbf{g}_j < \mathbb{E}[\mathbf{g}_j] \end{cases}$$

and $\mathbf{z}^{(j)}$, with elements

$$(A.5) \quad \mathbf{z}_i^{(j)} = \sum_{l=1}^i \mathbf{y}_l^{(j)} + \sum_{l=i+1}^{e_j} \mathbf{q}_l^{(j)}$$

where e_j is the total number of elements in the vector $\mathbf{q}^{(j)}$. The index h_j is calculated as the minimum value of i satisfying $\mathbf{z}_i^{(j)} \geq \mathbf{g}_j$ if $\mathbf{g}_j > E[\mathbf{g}_j]$, and $\mathbf{z}_i^{(j)} \leq \mathbf{g}_j$ if $\mathbf{g}_j < E[\mathbf{g}_j]$. The adjusted probabilities are then calculated as

$$(A.6) \quad \mathbf{q}_i^{(j)'} = \begin{cases} \mathbf{y}_i^{(j)} & i < h_j \\ \mathbf{g}_j - \sum_{l=1}^{h_j} \mathbf{y}_l^{(j)} - \sum_{l=h+1}^{e_k} \mathbf{q}_l^{(j)} & i = h_j \\ \mathbf{q}_i^{(j)} & i > h_j \end{cases}$$

This particular approach was chosen to minimize the number of probabilities to be recalculated. Only the first h_j elements of $\mathbf{y}^{(j)}$ and $\mathbf{z}^{(j)}$ are needed, and $\mathbf{z}^{(j)}$ need not be explicitly calculated in practice.

Finally, after calculating the adjusted probabilities, we sample \mathbf{g}_j elements according to the pivotal scheme in Algorithm A.2.

A.3. Comparing compression schemes. In this work, we focus primarily on pivotal compression due to its optimality properties as discussed in Section 5.2. However, the optimality condition in Proposition 5.2 applies only to the error incurred in a single compression operation rather than the overall error for eigenvalue estimates obtained by subspace iteration with repeated compressions. In order to provide a sense of how pivotal compression performs in the context of randomized subspace iteration, we report numerical comparisons to two other compression schemes we have investigated previously, namely multinomial and systematic compression [22]. In the multinomial scheme, no elements are preserved exactly: instead, the compressed vector is constructed by independently sampling indices from the input vector with weights proportional to the magnitudes of the corresponding elements. In systematic compression, some elements are preserved exactly according to the same criterion as for pivotal compression ((3.1) and (3.2)), and the remaining elements are sampled using a systematic scheme.

Figure 4 presents results obtained by applying our randomized subspace iteration with each of these compression schemes to the Ne system described above. All estimates were obtained from trajectories with 50,000 iterations, with the burn-in time i_{\min} chosen as 20,000. Biases from the randomized subspace iteration scheme with multinomial compression are approximately 7 orders of magnitude greater than those from the systematic and pivotal schemes. Because the compression schemes themselves are unbiased, we attribute the greater biases in randomized subspace iteration with multinomial compression to increased statistical errors incurred at each iteration when performing multinomial compression. This is reflected in the variance associated with these estimates, which is approximately 50 times greater for the multinomial scheme than for systematic. Biases from the systematic and pivotal schemes were approximately the same, while estimates from the pivotal scheme exhibit approximately 3.5 times less variance. These results provide further justification for our use of pivotal resampling in our compression scheme.

Appendix B. Stability analysis of numerical experiments.

Plots of the condition number of the matrix $\mathbf{U}^* \mathbf{X}^{(i)}$ can be used to monitor the stability of calculations as the iteration proceeds. An increasing trend in the condition

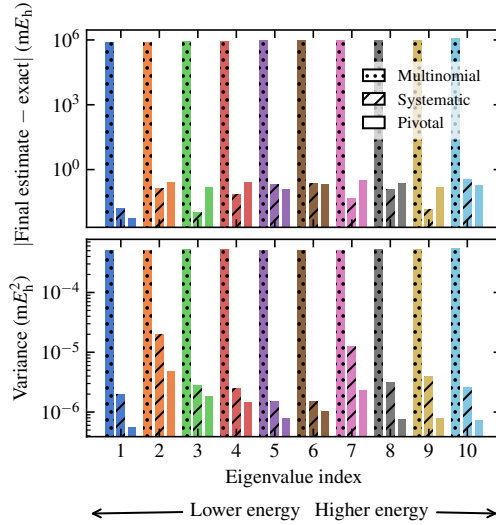


FIG. 4. Results obtained by applying our randomized subspace iteration with three different compression schemes (multinomial, systematic, and pivotal) to estimate eigenvalues for the Ne atom. In all schemes, iterate matrices were compressed to $m = 10,000$ nonzero elements per column. (top) The magnitude of the bias for each estimate, obtained from a trajectory of 50,000 iterations (with $i_{\min} = 20,000$). (bottom) The variance for each estimate, obtained using (5.67). Note the logarithmic scale on the vertical axes.

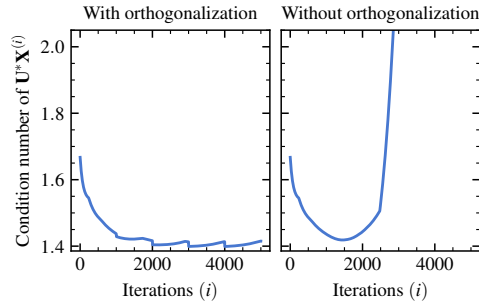


FIG. 5. The condition number of the matrix $\mathbf{U}^* \mathbf{X}^{(i)}$ at each iteration i of deterministic subspace iteration calculations on the Ne atom, either performing orthogonalization every 1000 iterations (left) or not at all (right).

number can indicate that orthogonalization is being performed too infrequently. In order to illustrate this, we present plots of this condition number obtained by applying two versions of deterministic subspace iteration to the Ne system introduced in Section 6.1. In the calculation shown in the left panel of Figure 5, orthogonalization was performed at intervals of 1000 iterations, while in the right panel, orthogonalization was not performed at all. Although both of these calculations yielded the same eigenvalue estimates, condition numbers in the calculation without orthogonalization increase rapidly, which suggests that the algorithm would encounter numerical instabilities if run for more iterations. After 5000 iterations, the condition number for this calculation is 59. In contrast, condition numbers in the calculation with orthogonalization remain less than 1.5.

Similarly, we monitored condition numbers for each calculation performed with our randomized subspace iteration (Sections 6.2 and 6.3). These are presented in Figure 6. In all cases, except for stretched C_2 , the condition number stabilized in the later stages of the iteration. A gradual increasing trend was observed at later iterations for stretched C_2 . We anticipate that this condition number would stabilize after more iterations and that the increase observed here did not affect the accuracy of our results, especially considering their close agreement with the numerically exact eigenvalues.

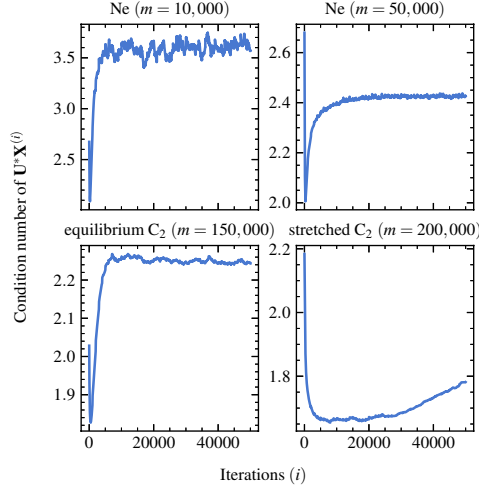


FIG. 6. The condition number of $\mathbf{U}^* \mathbf{X}^{(i)}$ at each iteration i for each of the randomized calculations presented in the main text.

Appendix C. Randomization of standard subspace iteration fails. This section describes the application of repeated stochastic sparsification techniques to a more standard subspace iteration, namely one that relies more upon nonlinear operations on the iterates $\mathbf{X}^{(i)}$. By comparing this “nonlinear” approach to the method in the main text (here referred to as “linear randomized subspace iteration”), we further elucidate the advantages of the non-standard features of linear randomized subspace iteration. Unlike in the linear approach, multiplication by $\mathbf{G}^{(i)}$ enforces orthonormality in the full n -dimensional vector space. At regular intervals, $\mathbf{G}^{(i)}$ is constructed from a Gram-Schmidt orthogonalization of the iterate columns. In other iterations, $\mathbf{G}^{(i)}$ is a diagonal matrix containing the ℓ_1 -norms of the iterate columns. As in our randomized calculations, we performed orthogonalization at intervals of 1000 iterations.

In each iteration, eigenvalues are estimated by applying the Rayleigh-Ritz method to the compressed iterate $\Phi(\mathbf{X}^{(i)})$, i.e. by solving the generalized eigenvalue equation

$$(C.1) \quad \Phi(\mathbf{X}^{(i)})^* \mathbf{A} \Phi(\mathbf{X}^{(i)}) \mathbf{W}^{(i)} = \Phi(\mathbf{X}^{(i)})^* \Phi(\mathbf{X}^{(i)}) \mathbf{W}^{(i)} \mathbf{\Lambda}^{(i)}$$

for the matrix $\mathbf{\Lambda}^{(i)}$ of Ritz values. Because this equation involves quadratic inner products of the compressed iterates, the resulting eigenvalue estimates are variational. Applying this approach with iterates compressed to $m = 10,000$ to the Ne system defined in the main text yields the eigenvalue estimates presented in Fig. 7. The

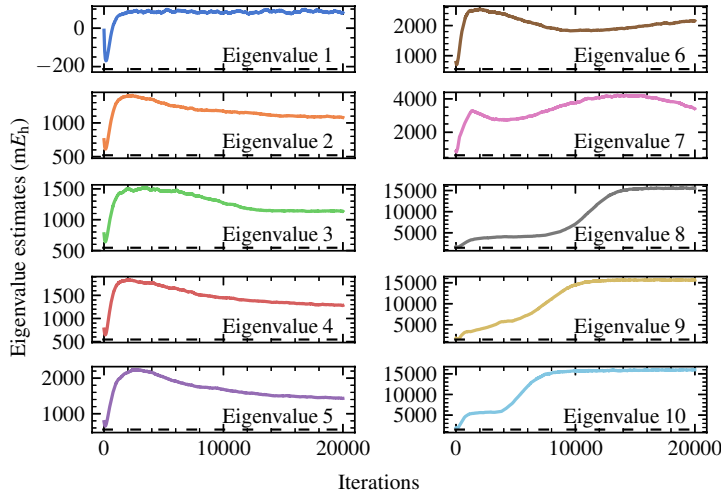


FIG. 7. **Eigenvalue estimates from randomizing a standard subspace iteration.** Estimates of the ten least-energy eigenvalues for Ne were obtained by compressing iterate matrices to $m = 10,000$ nonzero elements per column. Note the significantly greater errors relative to our randomized non-standard subspace iteration (Fig. 2). Dashed lines indicate exact eigenvalues.

best (i.e. minimum) estimates differ from the exact eigenvalues by as much as $201 mE_h$, indicating that the spans of the individual iterate matrices differ greatly from the dominant eigenspace of \mathbf{A} .

One might expect that averaging can be used to improve the accuracy of these eigenvalue estimates. However, because this approach is variational, averaging the Ritz values themselves yields estimates with at least as much error as the minimum eigenvalue estimates considered above. Instead averaging the $k \times k$ matrices $\Phi(\mathbf{X}^{(i)})^* \mathbf{A} \Phi(\mathbf{X}^{(i)})$ and $\Phi(\mathbf{X}^{(i)})^* \Phi(\mathbf{X}^{(i)})$, in analogy to linear randomized subspace iteration, yields poorer estimates. These differ from the exact eigenvalues by 299 to $10,590 mE_h$. Although the computational costs and memory requirements for this nonlinear approach are approximately the same as for the method in the main text, it is impossible to extract eigenvalue estimates of similar accuracy. This underscores the importance of the variance reduction techniques applied in our randomized subspace iteration.

Previous methods have sought to reduce the variance of estimated eigenvalues in alternative ways. For example, the bias could potentially be reduced by replacing one instance of the iterate matrix in (C.1) by an independently generated replica trajectory and omitting the orthogonalization step. This strategy has been tested previously in the context of the FCI problem [6]. However, as we have already mentioned, the variance in the inner products between uncorrelated vectors from independent trajectories can scale unfavorably with the matrix dimension n . An alternative is introduced in [11] in the context of the continuous space diffusion Monte Carlo algorithm. That scheme is an early instance of an algorithm often referred to as the Variational Approach to Conformal dynamics (VAC) [41, 61, 35]. In both the independent replica approach and in VAC, one needs to select a “time-lag” parameter sufficiently long to avoid bias due to the imperfect choice of trial vectors, but sufficiently short to avoid collapse to the dominant eigenvector. The difficulty in tuning the lag-time parameter

is one challenge that may hinder the application of these techniques.

Appendix D. Data Availability. All data from the numerical experiments presented here is available at <https://doi.org/10.5281/zenodo.4624477>. The code used to perform our numerical experiments can be accessed at <https://github.com/sgreene8/FRIES>.

Acknowledgments. We gratefully acknowledge productive discussions with Aaron Dinner, Michael Lindsey, Verena Neufeld, and James Smith throughout the development and execution of this project. Lek-Heng Lim originally raised the possibility of randomizing subspace iteration to us. Benjamin Pritchard provided invaluable suggestions for improving the readability and efficiency of our source code. Computational resources were provided by the Research Computing Center at the University of Chicago and the High Performance Computing Center at New York University.

REFERENCES

- [1] *Fast randomized iteration for electronic structure (FRIES)*, 2021. <https://github.com/sgreene8/FRIES> (accessed May 4, 2021).
- [2] H. ABDI AND L. J. WILLIAMS, *Principal component analysis*, WIREs Computational Statistics, 2 (2010), pp. 433–459, <https://doi.org/https://doi.org/10.1002/wics.101>, <https://onlinelibrary.wiley.com/doi/abs/10.1002/wics.101>.
- [3] A. ANDONI, R. KRAUTHGAMER, AND Y. POGROW, *On solving linear systems in sublinear time*, in 10th Innovations in Theoretical Computer Science Conference (ITCS 2019), A. Blum, ed., vol. 124 of Leibniz International Proceedings in Informatics (LIPIcs), Dagstuhl, Germany, 2018, Schloss Dagstuhl–Leibniz-Zentrum fuer Informatik, pp. 3:1–3:19, <https://doi.org/10.4230/LIPIcs.ITCS.2019.3>, <http://drops.dagstuhl.de/opus/volltexte/2018/10096>.
- [4] F. M. BICKELHAUPT AND E. J. BAERENDS, *Kohn-Sham Density Functional Theory: Predicting and Understanding Chemistry*, vol. 15, John Wiley & Sons, Ltd, New York, 2000, pp. 1–86, <https://doi.org/https://doi.org/10.1002/9780470125922.ch1>, <https://onlinelibrary.wiley.com/doi/abs/10.1002/9780470125922.ch1>.
- [5] N. S. BLUNT, A. ALAVI, AND G. H. BOOTH, *Krylov-projected quantum Monte Carlo method*, Phys. Rev. Lett., 115 (2015), p. 050603, <https://doi.org/10.1103/PhysRevLett.115.050603>, <http://link.aps.org/doi/10.1103/PhysRevLett.115.050603>.
- [6] N. S. BLUNT, A. ALAVI, AND G. H. BOOTH, *Nonlinear biases, stochastically sampled effective Hamiltonians, and spectral functions in quantum Monte Carlo methods*, Phys. Rev. B, 98 (2018), p. 085118, <https://doi.org/10.1103/PhysRevB.98.085118>, <https://link.aps.org/doi/10.1103/PhysRevB.98.085118>.
- [7] N. S. BLUNT, S. D. SMART, G. H. BOOTH, AND A. ALAVI, *An excited-state approach within full configuration interaction quantum Monte Carlo*, J. Chem. Phys., 143 (2015), p. 134117, <https://doi.org/10.1063/1.4932595>, <http://arxiv.org/abs/1508.04680>{%}0Ahttp://dx.doi.org/10.1063/1.4932595.
- [8] N. S. BLUNT, A. J. THOM, AND C. J. SCOTT, *Preconditioning and perturbative estimators in full configuration interaction quantum Monte Carlo*, J. Chem. Theory Comput., 15 (2019), pp. 3537–3551, <https://doi.org/10.1021/acs.jctc.9b00049>.
- [9] M. BOGOJESKI, L. VOGT-MARANTO, M. E. TUCKERMAN, K.-R. MÜLLER, AND K. BURKE, *Quantum chemical accuracy from density functional approximations via machine learning*, Nat. Commun., 11 (2020), p. 5223, <https://doi.org/10.1038/s41467-020-19093-1>.
- [10] G. H. BOOTH, S. D. SMART, AND A. ALAVI, *Linear-scaling and parallelisable algorithms for stochastic quantum chemistry*, Mol. Phys., 112 (2014), pp. 1855–1869, <https://doi.org/10.1080/00268976.2013.877165>, <http://www.tandfonline.com/doi/abs/10.1080/00268976.2013.877165>.
- [11] D. M. CEPERLEY AND B. BERNU, *The calculation of excited state properties with quantum Monte Carlo*, J. Chem. Phys., 89 (1988), pp. 6316–6328, <https://doi.org/10.1063/1.455398>, <http://aip.scitation.org/doi/10.1063/1.455398>.
- [12] G. CHAUVET, *On a characterization of ordered pivotal sampling*, Bernoulli, 18 (2012), pp. 1320–1340, <http://www.jstor.org/stable/41714093>.

- [13] G. CHAUVET, *A comparison of pivotal sampling and unequal probability sampling with replacement*, Statistics and Probability Letters, 121 (2017), pp. 1–5, <https://doi.org/https://doi.org/10.1016/j.spl.2016.09.027>, <http://www.sciencedirect.com/science/article/pii/S0167715216302024>.
- [14] J. D. CHODERA, *A simple method for automated equilibration detection in molecular simulations*, J. Chem. Theory Comput., 12 (2016), pp. 1799–1805, <https://doi.org/10.1021/acs.jctc.5b00784>, <http://pubs.acs.org/doi/10.1021/acs.jctc.5b00784>.
- [15] D. CLELAND, G. H. BOOTH, AND A. ALAVI, *Communications: Survival of the fittest: Accelerating convergence in full configuration-interaction quantum Monte Carlo*, J. Chem. Phys., 132 (2010).
- [16] E. U. CONDON, *The theory of complex spectra*, Phys. Rev., 36 (1930), pp. 1121–1133, <https://doi.org/10.1103/PhysRev.36.1121>, <https://link.aps.org/doi/10.1103/PhysRev.36.1121>.
- [17] E. R. DAVIDSON, *The iterative calculation of a few of the lowest eigenvalues and corresponding eigenvectors of large real-symmetric matrices*, J. Comput. Phys., 17 (1975), pp. 87–94, [https://doi.org/https://doi.org/10.1016/0021-9991\(75\)90065-0](https://doi.org/https://doi.org/10.1016/0021-9991(75)90065-0), <http://www.sciencedirect.com/science/article/pii/0021999175900650>.
- [18] J.-C. DEVILLE AND Y. TILLÉ, *Unequal probability sampling without replacement through a splitting method*, Biometrika, 85 (1998), pp. 89–101, <https://doi.org/10.1093/biomet/85.1.89>, <https://doi.org/10.1093/biomet/85.1.89>, <https://arxiv.org/abs/https://academic.oup.com/biomet/article-pdf/85/1/89/657024/85-1-89.pdf>.
- [19] J. FELDT AND C. FILIPPI, *Excited-state calculations with quantum Monte Carlo*. Preprint at <http://arxiv.org/abs/2002.03622>, feb 2020, <http://arxiv.org/abs/2002.03622>. (accessed May 4, 2021).
- [20] D. FOREMAN-MACKEY, D. W. HOGG, D. LANG, AND J. GOODMAN, *emcee: The MCMC Hammer*. Preprint at <https://arxiv.org/abs/1202.3665>, 2013, <https://doi.org/10.1086/670067>, <https://arxiv.org/abs/1202.3665>. (accessed May 4, 2021).
- [21] A. GREENBAUM, R.-C. LI, AND M. L. OVERTON, *First-order perturbation theory for eigenvalues and eigenvectors*, SIAM review, 62 (2020), pp. 463–482.
- [22] S. M. GREENE, R. J. WEBBER, J. WEARE, AND T. C. BERKELBACH, *Beyond walkers in stochastic quantum chemistry: Reducing error using fast randomized iteration*, J. Chem. Theory Comput., 15 (2019), pp. 4834–4850, <https://doi.org/10.1021/acs.jctc.9b00422>, <http://pubs.acs.org/doi/10.1021/acs.jctc.9b00422>.
- [23] S. M. GREENE, R. J. WEBBER, J. WEARE, AND T. C. BERKELBACH, *Improved fast randomized iteration approach to full configuration interaction*, J. Chem. Theory Comput., 16 (2020), pp. 5572–5585, <https://doi.org/10.1021/acs.jctc.0c00437>, <https://doi.org/10.1021/acs.jctc.0c00437>.
- [24] M. GU, *Subspace iteration randomization and singular value problems*, SIAM Journal on Scientific Computing, 37 (2015), pp. A1139–A1173.
- [25] A. GUT, *Probability: a graduate course*, vol. 75, Springer Science & Business Media, 2013.
- [26] N. HALKO, P.-G. MARTINSSON, Y. SHKOLNISKY, AND M. TYGERT, *An algorithm for the principal component analysis of large data sets*, SIAM Journal on Scientific computing, 33 (2011), pp. 2580–2594.
- [27] N. HALKO, P.-G. MARTINSSON, AND J. A. TROPP, *Finding structure with randomness: Probabilistic algorithms for constructing approximate matrix decompositions*, SIAM review, 53 (2011), pp. 217–288.
- [28] H. JI, M. MASCAGNI, AND Y. LI, *Convergence analysis of Markov chain Monte Carlo linear solvers using Ulam–von Neumann algorithm*, SIAM J. Numer. Anal., 51 (2013), pp. 2107–2122, <https://doi.org/10.1137/130904867>, <https://doi.org/10.1137/130904867>.
- [29] G. L. JONES ET AL., *On the markov chain central limit theorem*, Probability surveys, 1 (2004), pp. 299–320.
- [30] P. KNOWLES AND N. HANDY, *A new determinant-based full configuration interaction method*, Chem. Phys. Lett., 111 (1984), pp. 315–321, [https://doi.org/10.1016/0009-2614\(84\)85513-X](https://doi.org/10.1016/0009-2614(84)85513-X), <http://linkinghub.elsevier.com/retrieve/pii/000926148485513X>.
- [31] A. KNYAZEV, *Sharp a priori error estimates of the rayleigh-ritz method without assumptions of fixed sign or compactness*, Mathematical notes of the Academy of Sciences of the USSR, 38 (1985), pp. 998–1002.
- [32] M. H. KOLODRUBETZ, J. S. SPENCER, B. K. CLARK, AND W. M. C. FOULKES, *The effect of quantization on the full configuration interaction quantum monte carlo sign problem*, The Journal of chemical physics, 138 (2013), p. 024110.
- [33] C. LANCZOS, *An iteration method for the solution of the eigenvalue problem of linear differential and integral operators*, J. Res. Natl. Bur. Stand., 45 (1950), pp. 255–282.
- [34] L.-H. LIM AND J. WEARE, *Fast randomized iteration: Diffusion Monte Carlo through the lens*

- of numerical linear algebra, SIAM Rev., 59 (2017), pp. 547–587, <https://doi.org/10.1137/15M1040827>, <http://epubs.siam.org/doi/10.1137/15M1040827>.
- [35] C. LORPAIBOON, E. H. THIEDE, R. J. WEBBER, J. WEARE, AND A. R. DINNER, *Integrated variational approach to conformational dynamics: A robust strategy for identifying eigenfunctions of dynamical operators*, J. Phys. Chem. B, 124 (2020), pp. 9354–9364.
 - [36] J. LU AND Z. WANG, *The full configuration interaction quantum Monte Carlo method in the lens of inexact power iteration*. Preprint at <https://arxiv.org/abs/1711.09153> (2017), <https://arxiv.org/abs/1711.09153>. (accessed May 4, 2021).
 - [37] S. P. MEYN AND R. L. TWEEDIE, *Markov chains and stochastic stability*, Springer Science & Business Media, 2012.
 - [38] M. MOTTA AND S. ZHANG, *Ab initio computations of molecular systems by the auxiliary-field quantum Monte Carlo method*, Wiley Interdiscip. Rev.: Comput. Mol. Sci., (2018), p. 1364, <https://doi.org/10.1002/wcms.1364>, <https://onlinelibrary.wiley.com/doi/pdf/10.1002/wcms.1364>.
 - [39] C. MUSCO AND C. MUSCO, *Randomized block krylov methods for stronger and faster approximate singular value decomposition*, arXiv preprint arXiv:1504.05477, (2015).
 - [40] M. P. NIGHTINGALE AND H. W. J. BLÖTE, *Transfer-matrix Monte Carlo estimates of critical points in the simple-cubic ising, planar, and Heisenberg models*, Phys. Rev. B, 54 (1996), pp. 1001–1008, <https://doi.org/10.1103/PhysRevB.54.1001>, <https://link.aps.org/doi/10.1103/PhysRevB.54.1001>.
 - [41] F. NOÉ AND F. NÜSKE, *A variational approach to modeling slow processes in stochastic dynamical systems*, Multiscale Model. Simul., 11 (2013), pp. 635–655, <https://doi.org/10.1137/110858616>, <https://doi.org/10.1137/110858616>.
 - [42] Y. OHTSUKA AND S. NAGASE, *Projector Monte Carlo method based on Slater determinants: Test application to singlet excited states of H₂O and LiF*, Chem. Phys. Lett., 485 (2010), pp. 367 – 370, <https://doi.org/https://doi.org/10.1016/j.cplett.2009.12.047>, <http://www.sciencedirect.com/science/article/pii/S0009261409015607>.
 - [43] C. OVERY, G. H. BOOTH, N. S. BLUNT, J. J. SHEPHERD, D. CLELAND, AND A. ALAVI, *Unbiased reduced density matrices and electronic properties from full configuration interaction quantum Monte Carlo*, J. Chem. Phys., 141 (2014), p. 244117, <https://doi.org/10.1063/1.4904313>, <http://aip.scitation.org/doi/10.1063/1.4904313>.
 - [44] A. OZDAGLAR, D. SHAH, AND C. L. YU, *Asynchronous approximation of a single component of the solution to a linear system*, IEEE Trans. Netw. Sci. Eng., 7 (2019), pp. 975–986.
 - [45] B. N. PARLETT, *The symmetric eigenvalue problem*, SIAM, 1998.
 - [46] F. R. PETRUZIELLO, A. A. HOLMES, H. J. CHANGLANI, M. P. NIGHTINGALE, AND C. J. UMRIGAR, *Semistochastic projector Monte Carlo method*, Phys. Rev. Lett., 109 (2012), p. 230201, <https://doi.org/10.1103/PhysRevLett.109.230201>, <https://link.aps.org/doi/10.1103/PhysRevLett.109.230201>.
 - [47] M. REED AND B. SIMON, *Methods of modern mathematical physics. vol. 4. operator analysis*, 1979.
 - [48] V. ROKHLIN, A. SZLAM, AND M. TYGERT, *A randomized algorithm for principal component analysis*, SIAM Journal on Matrix Analysis and Applications, 31 (2010), pp. 1100–1124.
 - [49] Y. SAAD, *Numerical Methods for Large Eigenvalue Problems*, Society for Industrial and Applied Mathematics, 2nd ed., 2011, <https://books.google.com/books?id=FAkNAQAIAAJ>.
 - [50] J. C. SLATER, *The theory of complex spectra*, Phys. Rev., 34 (1929), pp. 1293–1322, <https://doi.org/10.1103/PhysRev.34.1293>, <https://link.aps.org/doi/10.1103/PhysRev.34.1293>.
 - [51] G. L. G. SLEIJPEN AND H. A. VAN DER VORST, *A Jacobi-Davidson iteration method for linear eigenvalue problems*, SIAM J. Matrix Anal. Appl., 17 (1996), pp. 401–425, <https://doi.org/10.1137/S0895479894270427>, <http://epubs.siam.org/doi/10.1137/S0895479894270427>.
 - [52] A. SOKAL, *Monte Carlo methods in statistical mechanics: Foundations and new algorithms*, in Functional Integration, C. DeWitt-Morette, P. Cartier, and A. Folacci, eds., vol. 351 of NATO ASI Series (Series B: Physics), Springer, Boston, MA, 1997, pp. 131–192, https://doi.org/10.1007/978-1-4899-0319-8_6, http://link.springer.com/10.1007/978-1-4899-0319-8_{_}6.
 - [53] J. SPENCER, N. BLUNT, AND W. FOULKES, *The sign problem and population dynamics in the full configuration interaction quantum monte carlo method*, The Journal of chemical physics, 136 (2012), p. 054110.
 - [54] J. S. SPENCER, N. S. BLUNT, AND W. M. FOULKES, *The sign problem and population dynamics in the full configuration interaction quantum Monte Carlo method*, J. Chem. Phys., 136 (2012), p. 054110, <https://doi.org/10.1063/1.3681396>, <http://aip.scitation.org/doi/10.1063/1.3681396>.
 - [55] G. STEWART, *Methods of simultaneous iteration for calculating eigenvectors of matrices*,

- in Topics in Numerical Analysis II, J. J. Miller, ed., Academic Press, 1975, pp. 185 – 196, <https://doi.org/https://doi.org/10.1016/B978-0-12-496952-0.50023-4>, <http://www.sciencedirect.com/science/article/pii/B9780124969520500234>.
- [56] G. W. STEWART, *Accelerating the orthogonal iteration for the eigenvectors of a Hermitian matrix*, Numer. Math., 13 (1969), pp. 362–376, <https://doi.org/10.1007/BF02165413>.
 - [57] G. W. STEWART, *Volume I: Basic Decompositions*, Matrix Algorithms, Society for Industrial and Applied Mathematics, Philadelphia, PA, 1998.
 - [58] G. W. STEWART, *Volume II: Eigensystems*, Matrix Algorithms, Society for Industrial and Applied Mathematics, Philadelphia, PA, 2001.
 - [59] Q. SUN, T. C. BERKELBACH, N. S. BLUNT, G. H. BOOTH, S. GUO, Z. LI, J. LIU, J. D. MCCLAIN, E. R. SAYFUTYAROVA, S. SHARMA, S. WOUTERS, AND G. K.-L. CHAN, *PySCF: the Python-based simulations of chemistry framework*, Wiley Interdiscip. Rev.: Comput. Mol. Sci., 8 (2018), p. e1340, <https://doi.org/10.1002/wcms.1340>, <http://doi.wiley.com/10.1002/wcms.1340>.
 - [60] W. A. VIGOR, J. S. SPENCER, M. J. BEARPARK, AND A. J. W. THOM, *Understanding and improving the efficiency of full configuration interaction quantum Monte Carlo*, J. Chem. Phys., 144 (2016), p. 094110, <https://doi.org/10.1063/1.4943113>, <http://aip.scitation.org/doi/10.1063/1.4943113>.
 - [61] R. J. WEBBER, E. H. THIEDE, D. DOW, A. R. DINNER, AND J. WEARE, *Error bounds for dynamical spectral estimation*, SIAM Journal on Mathematics of Data Science, 3 (2021), pp. 225–252.
 - [62] M. O. WILLIAMS, I. G. KEVREKIDIS, AND C. W. ROWLEY, *A data-driven approximation of the Koopman operator: Extending dynamic mode decomposition*, J. Nonlinear Sci., 25 (2015), pp. 1307–1346.
 - [63] S. WOLD, K. ESBENSEN, AND P. GELADI, *Principal component analysis*, Chemom. Intell. Lab. Syst., 2 (1987), pp. 37–52, [https://doi.org/https://doi.org/10.1016/0169-7439\(87\)80084-9](https://doi.org/https://doi.org/10.1016/0169-7439(87)80084-9), <https://www.sciencedirect.com/science/article/pii/0169743987800849>. Proceedings of the Multivariate Statistical Workshop for Geologists and Geochemists.